

Landslide Hazard and Erosion Susceptibility Assessment

Tarboo-Dabob Bay,
Washington

Prepared by
M2 Environmental Services
for
Northwest Watershed Institute
January, 2008

TARBOO-DABOB SLOPE STABILITY

Daniel Miller
M2 Environmental Services
3040 NW 57th Street,
Seattle, WA 98107-2551
206-783-0898

January 21, 2008



Daniel J. Miller

TARBOO-DABOB SLOPE STABILITY

SUMMARY

Purpose of Study

This study presents data and analyses to identify the source areas for landsliding and soil erosion that provide sediment and organic materials to Tarboo/Dabob Bay. This information is presented to aid decision makers in considering expansion of the existing Natural Area Preserve and creation of a new Natural Resource Conservation Area as part of ongoing efforts to protect the ecologic and economic resources provided by the bay.

The Natural Setting

Landsliding and soil erosion are natural processes that supply the raw materials of which bay environments are constructed and maintained. They provide the mud, sand, gravel, cobbles, and logs that form beaches, spits, and tidal flats, and the nutrients that support the plant and animal communities that utilize these environments. Landslides and erosion are triggered by high-intensity or long-duration rain storms, with much of the sediment delivered to stream channels then carried to the bay in accompanying high stream flows. Thus, most of the sediment delivered to the bay comes in pulses, in conjunction with large winter storms. The physical and biologic environment of the bay is finely attuned to the frequency and magnitude of these pulses; therefore an important aspect of assessing risks to the bay is consideration of human activities that alter the frequency and magnitude of sediment delivery.

The topography and geology of the Tarboo/Dabob Bay watershed reflect the profound legacy of continental glaciation. The watershed drains a several-hundred-foot thick layer of sediments deposited by streams draining the glacier, first as it advance southward and, thousands of years hence, as it retreated north. One consequence of this history is that rates of landsliding and soil erosion are acutely sensitive to activities that disrupt forest cover: the soils and underlying deposits have very low intrinsic cohesive strength. One step in assessing risks to the bay, therefore, is to identify areas where landslides and erosion can occur: these are the sites where human activities will alter natural rates of sediment production and delivery.

Approach and Results

This analysis uses an objective, automated procedure, based on locations of past landslide and erosional sites, to quantify susceptibility to these processes across the watershed.

Data consist of landslide locations and areas of persistent surface erosion mapped from aerial photographs of approximately 1:12,000 scale and high-resolution digital elevations (point

elevations over a 6-foot grid spacing) derived from laser altimetry (LiDAR). The analyses are designed to quantify susceptibility to landsliding and erosion in terms of the proportion of mapped sites included in defined hazard zones, based on correlations between observed locations of landsliding and erosion with topographic attributes of slope gradient and convergence. This strategy provides a consistent and objective method for identifying terrain subject to landsliding and surface erosion.

Based on this analysis, landslides occur on slopes greater than 55% and all slopes are subject to persistent erosion of exposed soils (see Figure 11). Within the project area, all slopes drain either directly to the bay or into streams that drain to the bay.

We have also used the digital data with an automated computer algorithm to identify terrain indicative of earthflows, a type of landslide involving gradual deep-seated movement of water-saturated soils, typically over an extent of an acre or more. When active, earthflows are characterized by numerous small slumps and bank failures into adjacent streams. Earthflow activity responds to changes in groundwater flow; thus earthflow movement varies in response to seasonal and annual variations in precipitation. Loss of forest cover increases the proportion of rainfall that infiltrates to recharge groundwater. Timber harvest or conversion of lands to non-timber uses can potentially cause movement at rates greater than would occur if the groundwater recharge zone to the earthflow were fully forested. Figure 12 shows areas identified as potential earthflow sites with estimated groundwater recharge zones to the sites.

Relationship to other Hazard-Mapping Programs

The Washington Department of Natural Resources also has two programs for identifying landslide-prone terrain: the slpstab slope stability screen, which provides a categorical hazard rating using techniques similar to those presented here, but with lower-resolution elevation data and without site-specific landslide mapping, and the Landslide Hazard Zonation Project, based on air-photo mapping and field recognizance to identify landslide-prone landforms. The results presented here are consistent with these other hazard-mapping programs, and augment their results with a high-resolution, calibrated ranking of shallow landslide and erosion susceptibility.

Recommendations

All these methods provide estimates of landslide hazard, which provide information about the relative likelihood for landsliding and soil erosion. A hazard can be defined, quantified, and mapped, as done here for shallow-rapid landsliding and soil erosion in terms of the proportion of mapped sites included within a given hazard level (or, as done with earthflows, in terms of the degree to which local topography is similar to that found on a single known example). Some judgment is now required to translate that hazard to implications for the resources we seek to protect. In the context of Tarboo/Dabob Bay, there is an important point to consider: all sediment produced in the watershed eventually ends up in the bay, which serves, therefore, as the focal point for the cumulative effects of human activities in the entire watershed. Any activity that

affects landslide and erosional susceptibility adds to a cumulative shift in the frequency and magnitude of sediment fluxes to the bay: the effects of any new activity are added on top of the persistent effects of all past activities.

The risk posed to the bay depends, therefore, both on the degree of susceptibility – the hazard level – and on the area encompassed. A large area with a low hazard rating can produce as many landslides as a small area with a high hazard rating, with the same consequences. If, for example, the goal is to eliminate human-induced changes to the frequency and magnitude of sediment delivery to the bay, human activities must be excluded from all areas with any potential for landsliding or erosion, shown in Figure 11, and for all areas that might potentially influence earthflow activity (Figure 12). If some level of human-induced change is deemed acceptable, then less restrictive guidelines can be established, using the information presented in Figures 9, 10, 12, and 15, and from the other hazard-mapping programs. However, there are no tools to translate hazard level to a quantified measure of ecological effects, so we can provide no hard guidelines to anticipate the consequences of a particular decision. This is why zero-tolerance of human-induced changes is sometimes advocated for highly valued resources.

These aspects of risk assessment also have bearing for on-site assessments. Ground-based evaluations can see details unresolved in a regional analysis, but do not incorporate the cumulative effects of other sites into an assessment of risk. Likewise, there are no guidelines for incorporating the value of the threatened resource into an assessment of risk. Timber harvest of a hillslope might be viewed more cautiously if there were a neighborhood of occupied homes at its base. Here we have Tarboo/Dabob Bay at the receiving end; the timing between landslide or erosion events and the response of the bay is indirect, so the nature of the risk is not readily apparent. Low risk, even with a field assessment, is still greater than no risk: given a big enough rainstorm, even the low-risk sites can fail, and the consequences should be evaluated in light of both cumulative effects and the importance of the resources potentially impacted.

One role of Natural Area Preserves and Natural Resources Conservation Areas is to protect native ecosystems, which includes protection of the processes that drive ecosystem function. For Tarboo/Dabob Bay, this involves maintaining sediment fluxes to the bay within natural ranges of frequency and magnitude, which ultimately requires protection of all areas susceptible to landsliding and soil erosion. Given the pattern of ownership and landuse within the basin, such widespread measures may not be feasible; yet any actions that limit human-induced changes to the erosion regime reduce the cumulative effects of all activities in the watershed, thereby helping to restore and maintain the resilience of the bay ecosystem in the face of continuing human activities elsewhere in the watershed.

INTRODUCTION

This report presents analyses to identify and quantify processes, locations, and relative rates of sediment production for Tarboo/Dabob Bay. The goal is to help evaluate the benefits of expanding an existing Natural Area Preserve and/or establishing a Natural Resource Conservation Area (NRCA) within the watershed to the bay, and for delineating the appropriate boundaries for any proposed action. This work focuses specifically on landsliding and soil erosion: the processes that transport sediment and organic material to the bay and to streams that drain to the bay. This sediment and organic debris provides the substrates and nutrients crucial to the aquatic ecosystem of the bay and its numerous tributaries. Landsliding and erosion of coastal bluffs, for example, provide beach sands, gravels, and large driftwood, without which there would be no spits to form Tarboo Bay. Landslide and erosion activity varies in response to large storm events, changing seasonal weather, and loss of forest cover. In the past, forests were lost to wildfire, wind, insect infestations, and disease. These losses were transient: forests grew back. We now suppress fires, but have added to the list timber harvest, road construction, and conversion of timberlands to agricultural and residential uses, some of which lead to permanent changes in forest cover. In changing the factors that control landslide and erosional processes, we have changed the rate, timing, and locations at which sediment and organic debris are delivered to the bay. Additionally, we have changed the nature of the materials delivered. It takes decades to grow a conifer of substantial size (> 36" dbh); landslides in areas clear-cut within the past century do not carry woody debris of the size carried by their predecessors.

The ecological consequences of these changes are not fully understood, but certain effects are readily observed. Because fine-grained sediments are flushed through streams as wash load, carried as the mud that makes water turbid, increased rates of landsliding and erosion show up first as deposition of mud and silt in the beds of channels feeding the bay and on the tidal flats that support, among other resources, a thriving oyster-farming industry. Mud and silt are an integral part of floodplain and estuarine environments, and the organisms that use these environments are well adapted to the inputs of mud and silt that have been carried by flood flows to the bay throughout the ten thousand years since the last ice sheet retreated. They are not well adapted, however, to deal with changes in the frequency and rate at which mud, silt, and associated organic materials are carried to the bay, with the consequence that actions in the watershed that affect erosional processes alter both the physical environment and associated ecosystem of the bay. One goal of an NRCA is to protect outstanding examples of native ecosystems. Protection of an ecosystem requires that the processes that drive ecosystem function operate within the regime of frequency and magnitude to which the ecosystem is adapted. Within the context of landsliding and soil erosion, a first step is to identify those sites where landslide and erosion processes are most sensitive to human activities. That is the goal with this work – to show where sediment is produced in this watershed and to identify areas where landuse activities can alter rates of sediment production.

For mapping over this extent (e.g., thousands of acres), we must rely primarily on information from remotely sensed data and existing maps, i.e., aerial photography, and topographic and geologic maps. Two basic approaches have been developed for slope-stability mapping at this scale: terrain mapping, which seeks to identify potentially unstable landforms, and computerized analyses using Geographic Information Systems (GIS), which seek correlations between landslide locations and topographic, geologic, vegetation, and other attributes for which data may be available. The Washington Department of Natural Resources Landslide Hazard Zonation Project, for example, takes the first approach, focusing on the identification and mapping of specific landforms and assignment of a hazard rating, based on observed landslide history, to each landform type. This provides a methodology consistent with the physical conditions that cause landsliding and the use of landforms provides a means of translating results from a map to on-the-ground interpretations. It relies, to some extent, on the ability of the mapper to identify and resolve landform types. I've taken the second approach, and seek to empirically quantify landslide susceptibility based on topographic attributes identified at the greatest detail provided by available data. I rely on computer-generated attributes, which provides a high degree of objectivity, and removes (for better or worse) the experience and ability of the analyst at recognizing signs of potential slope instability. For this study, digital elevation data obtained from laser altimetry (LiDAR, for Light Detection and Ranging) were available. These provide a level of topographic detail approaching (and for large areas, exceeding) that of ground-based surveys.

A STRATEGY FOR QUANTIFYING LANDSLIDE AND EROSION SUSCEPTIBILITY

Rates of soil erosion by landsliding and surface runoff are variable across the landscape, with typically larger magnitudes in areas of steeper topography and weaker material properties. Our goal is to empirically quantify spatial variability in these rates, by which we can then identify source areas for sediment and rank these areas in terms of their relative contribution to total sediment production. We do this by mapping landslide and surface erosion locations, overlaying these locations on digital maps of topography, soils, and geology, and then calculating landslide and erosion-site density (e.g., number of landslides per unit basin area) as functions of topographic attributes in different substrate types (e.g., areas underlain by bedrock versus areas underlain by unconsolidated glacial sediments). For example, mapped landslide initiation points can be overlain on a digital slope map to give landslide density (number of landslides per unit area) for different slope-gradient classes (e.g., 70-80% slopes). This gives the proportion of mapped landslides initiating within each slope class, which can be translated to a map delineating zones (based on slope) containing specified proportions of the landslide initiation sites.

Different landslide and erosional process are associated with different topographic attributes. For example, source areas for debris slides and debris flows (using the terminology of the WA DNR Landslide Hazard Zonation Project Protocol, Version 2.1), which involve the sudden failure of

shallow soils, occur in steep, and (in many cases, but not all) convergent terrain (e.g., bedrock hollows), whereas earthflows, which involve the slow downslope deformation of a large volume of material, are characterized by lower-gradient, hummocky terrain with disrupted drainage and ponds. Even for a single process, the important topographic attributes may differ depending on characteristics of the triggering event; in the San Francisco Bay area, Wieczorek (1987) for example, found that long-duration, moderate-intensity storms tended to trigger landslides on concave slopes at downslope locations with large contributing areas, whereas short-duration, high-intensity storms tended to trigger landslides from steep slopes with no contributing-area dependence. The analysis must be tailored for the types of processes occurring within the region of interest.

GEOMORPHIC SETTING

Our focus in this study is on the southern portion of the watershed to Tarboo Bay and the northern portion of Dabob Bay (Figure 1), which includes the southern end of Tarboo Creek and numerous small streams draining directly to the bay. The entire watershed covers about 14,460 acres and the project area includes the southern half of the watershed.

In the Puget lowlands, current erosional processes reflect the topographic and stratigraphic legacy of repeated continental glaciations (Booth et al. 2003). Bordered to the west by the Olympic Mountains and to the east by the Cascades, the Puget basin contains a low-relief plateau whose upper layers are composed largely of sediments deposited between 20,000 and 10,000 years ago during the last advance of the Puget Lobe of the cordilleran ice sheet. Melt water streams carrying sediment eroded by the ice flowed across a broad outwash plain and into proglacial lakes, leaving a thick sequence of sands and gravels interspersed with lake-bottom deposits. Current water bodies, both marine (Hood Canal) and fresh (Lake Washington), fill channels scoured by ice and water below the ice sheet (Booth and Hallet 1993). Likewise, modern rivers, including Tarboo Creek, follow courses established by ice-formed topography draining vast quantities of glacial melt water.

The Tarboo watershed exhibits all these glacially derived features: the bay occupies an extension of the Hood Canal, a sub-ice meltwater channel. The plateau surface here, as over much of the Puget Lowlands, is plastered with a thin layer of glacial till, a compact deposit formed at the base of the nearly mile-thick ice sheet. Elevation of the plateau surface extends up to about 600 feet, with topography characterized by a series of broad, parallel ridges and troughs (flutes) aligned with the north-south direction of ice-sheet flow. Tarboo Creek flows south to the bay through one of these troughs. Steep slopes, incised by a series of small channels, extend from the plateau surface to the bay and expose the underlying stratigraphy (Figure 2): typically, a 100-foot-thick layer of sands, gravels, and silts (outwash) overlay older deposits that, although laterally variable, tend to be silt rich.

This stratigraphy sets the stage for erosional processes in the watershed. The upper deposits are unconsolidated and easily eroded. They are also permeable, so precipitation readily infiltrates and, except for discharge from impermeable surfaces (roads), surface runoff is rare: as long as there is vegetation cover, there is little potential for surface erosion. However, these materials can be readily eroded by discharge of road drainage or where landsliding or human activities have removed vegetation on steep slopes. The underlying, silt-rich deposits are less permeable, which forces lateral groundwater flow in the overlying permeable deposits. Where the contact between these deposits is exposed on slopes, groundwater emerges at the surface as seeps and springs, which feed perennial channels. Groundwater flow directions are controlled, in part, by the location of these seeps; groundwater flow converges toward areas where surface drainage or mass wasting has eroded channels into the slopes (Dunne 1980). This process forms a feed-back mechanism for headward erosion of these channels: seepage erosion of the unconsolidated deposits can form steep-sided channels, which then fail by slumping. Surface drainage removes this failed material, followed by renewed seepage erosion and headward slumping. The rate of headward advance is then set by the rate at which failed material is removed by surface water.

The overlying, well-drained, unconsolidated sands and gravels, although lacking cohesion, exhibit high inter-particle friction and can maintain surface slopes as steep as 70% to 80%, as long as they are not saturated with water. High-intensity rainstorms, or drainage from roads, can saturate surface layers, potentially triggering shallow, rapid landsliding on steep slopes in this material. The underlying silt-rich deposits have been consolidated by the pressure of overlying deposits and ice, and can maintain steep, near-vertical slopes. However, because they are fine grained, water drains from these materials very slowly, so they are nearly always saturated. Pore-water pressures reduce their frictional strength and, once they fail, these materials can maintain slopes of only about 30%. At elevations below the contact, many of the small valleys to the bay are filled with landslide deposits composed of this fine-grained material. When saturated, these deposits deform and move downslope as earthflows. Generally, this motion is gradual, but changes in geometry or hydrology can accelerate rates of earthflow movement.

Topography indicative of large, deep-seated landslides (slumps) is widespread along the coastal bluffs and along the east fork of Tarboo Creek and its northern tributaries. Topographic evidence of such landslides includes steep (>60% slope), arcuate headscarps, linear topographic depressions (e.g., sag ponds) and benches, and low-gradient (<50% slope) hummocky terrain through the landslide body. Such landslides are sensitive to the geometry of the slope and are commonly triggered or reactivated by erosion of the toe (e.g., Miller and Sias 1998). Coastal bluffs may be eroded by wave erosion during storms, with the potential for triggering motion of these landslides. Likewise, channel incision or lateral channel migration into landslide toes can also trigger motion of these features. I saw no evidence of extensive bluff erosion or channel incision in the aerial photographs I examined, and saw no evidence of recent movement on any of these large landslides. Site-specific geotechnical reports evaluating proposed timber harvests in the watershed also cite lack of evidence of activity on the large, deep-seated landslide features

examined (Pierson 2004, Grizzel 2006). It is likely that these features initially formed under conditions that no longer exist, such as after loss of lateral support as the ice sheet retreated, or under conditions that occur very rarely, such as during high-intensity earthquakes. Lack of evidence for recent activity leaves us with no data to empirically quantify susceptibility of these features to renewed activity; hence I do not address them in this report. This does not imply that there is no hazard posed by these features: stream incision or lateral migration, or road construction, that alter slope geometry can potentially destabilize existing features and trigger renewed movement.

METHODS

Available Data

Topographic data were derived from a LiDAR-derived "bare-earth" digital elevation model (DEM). The DEM was acquired from the Puget Sound LiDAR Consortium (<http://pugetsoundlidar.ess.washington.edu>; see http://pugetsoundlidar.ess.washington.edu/lidardata/metadata/pslc2001/pslc2001-02_be_dem.htm for metadata). This DEM provides elevation values over a horizontal grid spacing of six feet.

Digital geologic data are available from the Department of Natural Resources, derived from mapping at a scale of 1:100,000 (<http://www.dnr.wa.gov/geology/dig100k.htm>).

Digital soils data are available from the National Resources Conservation Service (<http://soils.usda.gov>). These are based on 1:24,000-scale soils mapping.

The LiDAR bare-earth DEM provides the primary data source for the digital analyses reported here. The geologic and soils data show broad patterns in the spatial distribution of soil depths and substrate type, but lack the spatial resolution and detail available from the DEM. Because material properties affect surface topography, the DEM itself provides more detailed information about the spatial distribution of material types than available from the geologic and soils data. However, I do use the geologic data to separate substrates into two broad categories: deep glacial sediments and bedrock. There are very limited bedrock exposures within the study watershed, but there are bedrock exposures within the larger area over which the landslide inventory was performed.

Digital color National Agriculture Imagery Program (NAIP) orthophotos with 1-m resolution, derived from 2006 aerial photography, and a shaded relief image produced from the DEM were used as a base map for landslide mapping. The NAIP imagery is available from the University of Washington (<http://rocky2.ess.washington.edu/data/raster/naip/index.html>).

Mapping

Fresh-appearing landslide scars and locations of active surface erosion were mapped from 1:12,000-scale aerial photograph stereo pairs, viewed with magnifying binoculars using a Topcon stereoscope. Mapping was done directly to digital files using heads-up (on screen) digitizing, with 2006 NAIP orthophotos (1-m resolution) and a shaded relief image made from a LiDAR bare earth DEM (6-foot horizontal resolution) as base maps. Each mapped polygon was assigned a type (e.g., debris slide, earthflow). Photo series from 1957, 1979, 1997, and 2003 were examined.

Results of this study are based entirely on landslide mapping from aerial photographs and computer-generated terrain mapping done with high-resolution digital data. I spent one day on the ground to gain a general sense of topographic and stratigraphic relationships to landsliding in the basin. The high resolution (6-feet) of the digital elevation data provides precision comparable to that obtained from field landslide inventories; however, details of local stratigraphy and land use also important to landslide initiation are not visible with these data. Such details are also not available for regional predictions of landslide susceptibility, which must rely on regionally available data (i.e., the same digital data used to calibrate the model). Site-specific details, visible only with on-the-ground observations, must enter into site-specific assessments.

Quantification of Susceptibility

Susceptibility to shallow landslides and surface erosion was characterized in terms of spatial variability in density, i.e., the number of landslides or exposed-soil area per unit basin area. Density is empirically calibrated as a function of topographic attributes. These attributes can then be mapped (from the DEM) to delineate zones that encompass a given proportion of the observed landslides. To the extent that the observed landslides and erosional sites indicate the potential for future landsliding and erosion, these maps provide a quantitative measure of susceptibility.

For shallow landslides, each mapped landslide was related to specific topographic attributes at the inferred point (DEM cell) of landslide initiation. For surface erosion, topographic attributes for each DEM cell within the entire area of mapped exposed soils were used. Initiation points for shallow landslides were inferred as follows. The perimeter of each visible landslide scar was digitized as a polygon. Each polygon had an associated area, perimeter, and an average length and width. Within the upper portion of each landslide polygon, a search was performed for the DEM cell having the largest topographic attribute value (e.g., the greatest slope). This search extended from the upper-most elevation along the polygon edge to a downslope distance equal to one and one half times the average width of the polygon. The identified DEM cell within this area was then flagged as the initiating point for that landslide.

Densities were calculated using two sets of topographic attributes; 1) slope gradient S (change in elevation divided by horizontal distance) and 2) the product of slope gradient S and a measure of

topographic convergence b . The value of b for a cell was calculated as the integral of incoming flow direction projected over the circumference of a circle centered about the cell, which gives units of length (i.e., the contour length crossed by flow into the circle), divided by the diameter of the circle. For planar flow, its value is one; for convergent flow its value is greater than one, up to a maximum of 2π (no outgoing flow), and for divergent flow, its value is less than one, to a minimum of zero (no incoming flow). For high-resolution LiDAR DEMs, the grid spacing may be smaller than the characteristic length of the topographic features of interest. For example, the average width of a topographic hollow, and the corresponding area over which it controls convergent flow of shallow groundwater, may extend for several tens of feet; greater than the 6-foot point spacing of the DEM. Both slope S and topographic convergence b can be calculated for any length scale with no loss of topographic detail.

Slope S and the product Sb were divided into equal-width classes (e.g., 0-10% slope, 10-20%, etc). For each class, the number of landslide initiation points n and the watershed area A within the class were summed. For the i^{th} class, this gives a landslide density ρ_i :

$$\rho_i = n_i/A_i \quad (1)$$

When divided by the overall mean landslide density ρ_0 (the total number of landslides divided by the total study area), we obtain a topographic weighting term w_i for the i^{th} class:

$$w_i = \rho_i/\rho_0. \quad (2)$$

We call this a topographic weighting, because it effectively weights the mean landslide density to account for effects of local topography (Miller and Burnett 2007). For example, the number of landslides n expected over a given area is estimated as the product of density and area, i.e., for a mean landslide density ρ_0 over area A , $n = A \rho_0$. In terms of a DEM, we calculate area as a sum over cells, i.e., $n = \sum a \rho_0$, where a is the area of a single cell and the sum is over all cells in the watershed. Likewise, the number of landslides expected over any portion of the watershed is estimated as the sum over cells in that portion. With the topographic weighting term, we can modify this estimate to account for effects of local topography

$$n = \sum a w_j \rho_0 = a \rho_0 \sum w_j \quad (3)$$

where w_j is the w value of the j^{th} cell (based on the topographic attributes of that cell), and the sum is over all cells in the area of interest. To obtain a continuous function of the associated topographic attribute, we define w as a step-wise continuous linear function over each class, and set the value of w at the class endpoints to minimize the difference in the number of landslides counted and the number calculated for each class. In many cases, particularly with small sample sizes, we find that the number of landslides varies unevenly from bin to bin, with some bins containing no landslides. This produces a large variability in the relative landslide density from bin to bin. However, we expect that topographic controls on landslide location vary smoothly over the range of attribute values; the observed variability from bin to bin arises in part from

inadequacies of our sample. We also expect a weighting function to represent topographic controls should vary smoothly, so we define this function to be smooth and to also minimize the difference between the observed and predicted number of landslides in each bin. These functions provide an empirically calibrated weighting value for each DEM cell.

To translate topographic weighting to a measure of relative landslide susceptibility, we plot the proportion of mapped landslides against topographic weighting value. For example, if we find that 50% of the mapped landslide initiation points fall on topographic weighting values greater than 10, we can map out the area required to encompass 50% of the mapped landslides, starting with the least-stable slopes, by flagging all cells with weight values greater than 10.

This strategy can be extended to sub-portions of the study area and extrapolated to areas outside the study area. In these cases, instead of using mapped landslides, we use the topographic weighting model (Equation 3) to calculate an estimate of the total number of landslides expected over the entire area of interest, and again to calculate the proportion of that total found in areas within each topographic class. DEM cells having weight values greater than or equal to a value x are expected to contain a proportion of all landslides $P(x)$:

$$P(x) = \frac{\sum w(x-w_{\max})}{\sum w(0-w_{\max})}, \quad (4)$$

where $\sum w(x-w_{\max})$ indicates the sum of all weighting values greater than or equal to x , $\sum w(0-w_{\max})$ indicates the sum of weighting values for all cells in the area of interest, and w_{\max} is the maximum weight value for any cell.

In this way, the model can be calibrated in one area, and then applied in other, similar areas, or as we do here, calibrated over a large area and applied over a subarea that does not include all the mapped landslides.

The methodology described here using landslide density in terms of number per unit area can also be applied for density defined in terms of landslide (or exposed mineral soil, for surface erosion) area per unit basin area. In this case, the n_i in Equation 1 is replaced by pa_i , the area of the i^{th} mapped polygon.

Earth Flows

Susceptibility to the formation and movement of earthflows is difficult to quantify here because evidence of active earthflows may not be visible on aerial photographs. This leaves little empirical evidence for identifying topographic attributes associated with this erosional process. Nevertheless, earthflow terrain is visible on the ground, found in the small drainages (of which I visited two) to the bay starting at elevations near the stratigraphic contact between overlying permeable sands and underlying less-permeable, fine-grained materials. These locations commonly contain springs and boggy ground. Active earthflow terrain is identified by hummocky topography, with numerous small slumps of varying age and clumps of disturbed vegetation (Figure 3) on slopes with relatively low overall relief (~15% to 30% gradient).

I could find only one example of earthflow terrain in the aerial photographs examined, based on an extensive zone of disturbed vegetation visible in the 1979 photographs. Figure 4 shows this site both on the LiDAR-derived shaded relief image and on the 2006 color photography. By 2006, the vegetation no longer shows any indication of the activity 25 years earlier; however, the area within the mapped earthflow extent on the shaded relief image exhibits slightly rougher topography than the adjacent upslope area. McKean and Roering (2004) used surface roughness, measured using high-resolution LiDAR-derived elevation data, as an indicator of earthflow extent and level of activity for a site in New Zealand. Their study site was in sedimentary bedrock, very different lithology and terrain than found for the Tarboo watershed, but we can employ similar techniques with the high-resolution digital elevation data available here. Zones of high surface roughness will be insufficient here, however, to delineate earthflow terrain, because areas affected by other processes, such as shallow landsliding, also exhibit high surface roughness. Roering et al. (2005) used a combination of surface roughness and slope gradient to identify zones of potential deep-seated landsliding in the Tyee sandstone portion of the Oregon Coast Range. They found that deep-seated landslides typically exhibited a lower range of slopes and lower roughness than found for adjacent terrain. These studies suggest that we can use a combination of topographic attributes to identify sites of potentially active earthflow movement.

I have used a combination of factors:

- A measure of surface roughness, using direction cosine eigenvalue ratios (McKean and Roering 2004) over a length scale of 30 feet (a diameter of five 6-foot DEM cells). The mapped earthflow (Figure 4) exhibited roughness values greater than 4.5.
- A measure of surface gradient, averaged over a circular surface of 300-foot diameter. The earthflow terrain fell on gradients between 15% and 30%.
- A measure of topographic convergence (as described earlier) measured over a circular area of 300-foot diameter. The earthflow terrain had values between 1.18 and 3.0.
- Within areas mapped as older and undifferentiated glacial deposits (Figure 2), which are typically finer grained than the overlying outwash deposits.

I then calculated the proportion of area within a circular window of 300-foot radius that met the above criteria. This proportion indicates the degree to which sites across the watershed resemble the earthflow terrain identified.

RESULTS

Shallow Landslides

Landslides were mapped over an area of about 60,000 acres, including the Tarboo watershed. Twenty six shallow landslides were included in the landslide inventory. These landslides occurred on both relatively planar and convergent slopes, and at both upper and mid-slope locations. Digitized polygons for these landslides were overlain on GIS layers for slope and

topographic convergence determined from the LiDAR DEM over a length scale of 65 feet. To limit this analysis to non-road-related landslides, initiation points falling within 85 ft of a road were excluded from further analyses. Landslide initiation points (determined as described previously) fell on slope gradients spanning a range from 55.7% to 146% (Figure 5). (Slope gradients over this range were divided into 25 equal-width bins and the relative landslide density, Equation 2 (which gives a topographic weighting) calculated for each. A smooth function was interpolated from these values. The resulting weight function, with the observed and predicted number of landslides in each bin, are shown in Figure 6. This weight function was then applied to the Tarboo watershed to delineate the areas required to encompass the slope gradients associated with specified proportions of the landslide locations expected within the watershed.

The same analysis was performed using Sb , the product of slope gradient and topographic convergence. In this case, landslide initiation points fell on Sb values spanning the range from 0.59 to 1.79 (Figure 5) and the corresponding weighting function is shown in Figure 6. When we plot the proportion of the landslide-prone area (i.e., all areas with slope gradients greater than 55.7%) required to encompass a given proportion of the mapped landslides (Figure 7), the slope and convergence (Sb) criteria appears to better resolve topographic controls on landslide location, in that a greater proportion of the landslides are included in a smaller proportion of the area. It is important to note, however, that the most likely topographic locations for landsliding may vary with different storm characteristics (Wieczorek 1987). The inclusion of topographic convergence incorporates the effects of local focusing of shallow subsurface flow (e.g., Montgomery and Dietrich 1994), which may form an important control on landslide locations during long duration storms. However, short-duration, high-intensity periods of rainfall can create shallow, near-surface zones of high pore pressure (e.g., Iverson 2000) and trigger shallow landsliding on steep slopes regardless of the degree of topographic convergence. Thus, although the slope and convergence (Sb) based criteria appears to better resolve landslide locations (for this data set) than the slope-based criteria, it may underestimate the susceptibility of planar slopes to landslide initiation during high-intensity storms. Results from both criteria are therefore used to characterize susceptibility to shallow landsliding.

The weighting functions shown in Figure 6 were used to calculate a weighting value for each DEM cell. Cells were then ranked from smallest to largest weight values and, for each cell, Equation 4 was used to calculate the proportion of expected landslides with weight values less than or equal to that of the cell. Hence, a value of 1 indicates the highest level of susceptibility (all landslides are associated with weight values less than or equal to that of the cell), and the collection of cells with values between, say, 0.5 and 1.0 will contain 50% of all expected landslide sites. This method provides a logical measure of susceptibility: the landscape is delineated into the areas required to encompass a specified proportion of the mapped landslide sites (and to the degree that past landslides tell us where future landslides will occur, the expected landslide sites). It also allows us to combine estimates of susceptibility using different topographic criteria. For example, to combine calculations from the slope- and slope-with-

convergence-based criteria, we calculate the proportion with Equation 4 for each cell for each criterion, and then assign the cell the maximum proportion obtained. This result is shown for the Tarboo watershed in Figure 8 using three levels: starting with the least stable (most susceptible) sites, areas are delineated to encompass 50% (values from 1.0 to 0.5), 43% (values from 0.5 to 0.07) and 7% (values from greater than zero to 0.07) of the expected landslide initiation points. The 50% and 43% zones together include 93% of the mapped landslide initiation points, the same percentage included in the High hazard rating of the DNR slpstab slope stability screen, (Shaw and Vaugeois 1999). Together, these three zones include 100% of the expected landslide sites. Zones of high susceptibility to shallow landsliding are concentrated on steep, channel-adjacent slopes (inner gorges), steep headwall areas, deep-seated landslide headscarps, and on coastal bluffs.

Surface Erosion

Approximately 13 acres of exposed soils, interpreted as areas of surface erosion, were mapped from the aerial photos. These locations included DEM-inferred slopes from zero to 163%, and were used to define a slope-based topographic weighting function for surface erosion, shown in Figure 9. Equation 4 was used to define the proportion of DEM cells within mapped areas of surface erosion with weight values less than or equal to that of the cell. This provides a measure of susceptibility to surface erosion, mapped in Figure 10 to delineate the areas encompassing (as done for shallow landsliding) 50% (values from 1.0 to 0.5), 43% (values from 0.5 to 0.07) and 6% (values from 0.1 to 0.07) of the expected surface erosion sites.

Areas of inferred active surface erosion mapped from the aerial photographs extended to considerably lower surface gradients than found for landslide initiation sites. This may reflect my inability to differentiate zones of erosion from zones of deposition on the photos, and contributes to imprecision in our ability to resolve topographic controls on surface erosion using the DEM. However, these low-gradient areas composed a small proportion of the total area mapped, so their effect on the calibration is minor; all slopes less than 43% have weighting values less than one.

Combined Susceptibility for Sediment Production

Together, the susceptibility to shallow landsliding and susceptibility to surface erosion maps provide a spatially distributed measure of relative potential for sediment production from these related processes. Figure 11 shows the overlay of these two maps.

Earth Flows

The topographic criteria for delineating potential earthflow terrain were applied over the Tarboo watershed using the 6-foot-resolution LiDAR-derived DEM. Zones with greater than 25% and 50% of the area within a 150-foot radius meeting these criteria are shown in Figure 12. Also shown are the contributing areas to these zones based on flow directions inferred from the LiDAR DEM.

DISCUSSION

Comparison with State Department of Natural Resources Hazard Mapping

The Washington Department of Natural Resources has two programs for mapping of potential landslide hazards, the slpstab modeled slope stability screen (available at <http://www.dnr.wa.gov/forestpractices/data/> via the links to Slope Stability) and the Landslide Hazard Zonation Project (<http://www.dnr.wa.gov/forestpractices/lhzproject/>). The slpstab slope stability screen relies on a computer automated GIS-based model that uses DEM-inferred estimates of slope gradient and slope form (convergent, planar, and divergent), calibrated with regional landslide inventories (Shaw and Johnson 1995, Shaw and Vaugeois 1999). The Landslide Hazard Zonation Project is a watershed-specific analysis based on detailed aerial photograph landform and landslide mapping with ground-based validation.

Slpstab

The slpstab model uses the same strategy I used here for mapping susceptibility to shallow-rapid landslide initiation: correlate landslide density to topographic attributes by overlaying mapped landslide locations on digital topographic maps. Slpstab uses two topographic attributes, slope gradient and topographic curvature (a measure of slope form), calculated from the 10-m DEMs made by interpolation of elevations from contour lines on US Geological Survey 1:24,000-scale topographic maps. Values for these topographic attributes are divided into bins, forming a two-dimensional matrix (Table 2 in Shaw and Vaugeois 1999; gradients shown below are from their Table 6 for the Hazel Watershed, which contains glacial sediments similar to those in Tarboo):

Slope Curvature	Slope Gradient				
	Low -----High				
	15%	24%	47%	70%	Vertical
Convex (divergent)	Low	Low	Low	Low	Moderate
Planar	Low	Low	Low	Moderate	High
Concave (convergent)	Low	Moderate	High	High	High

The slpstab results (downloaded from the DNR web site listed above) for a portion of the Tarboo watershed are shown in Figure 13, along with results from this study. Shaw and Vaugeois (1999) state that, on average, a high-hazard rating in slpstab included at least some portion of 93% of the mapped landslides used to calibrate the model. Also shown in Figure 13 are the areas required to include 93% of the mapped landslide initiation sites and areas with exposed soils (surface erosion sites) used to calibrate the model used for this study. Both models recognize steep, convergent slopes in the amphitheater-like headwalls of the small drainages to the bay, steep slopes on head scarps to large deep-seated landslides, and steep slopes along the coastal bluffs as high-hazard zones. Important differences between these studies include:

- slpstab used elevation data on a 10-m (32.8 feet) grid; here I used data on a 1.8-m (6-foot) grid, which provides nearly 30 times more topographic data per unit area. Indeed, the spatial resolution provided by LiDAR provides detail similar to that obtained with a field topographic survey, but over a much larger area than feasible with on-the-ground measurements. Hence, we can now resolve topographic features such as inner gorges, which were not resolved on the 1:24,000-scale topographic maps or on the 10-m DEMs derived from those maps.
- The model presented here was calibrated with a landslide inventory from the Tarboo watershed and surrounding areas; such local data were not available for calibration of slpstab. Hence, these new results may better reflect local landslide processes.
- The algorithms used for this study allow delineation of hazard zones explicitly in terms of the proportion of mapped landslides included within each zone.

The high spatial density of elevation data available for this study allows finer resolution of landslide-prone topography. As seen in Figure 13, delineated high-hazard zones for shallow-rapid landsliding (93% of mapped landslides) are less extensive in headwall areas, focused in convergent topography, and more extensive along inner gorges. The high-hazard zone mapped for susceptibility to surface erosion more closely matches the extent of high-hazard zones mapped with slpstab. In fact, many of the exposed soils I mapped as persistent sites of surface erosion probably originated as landslide scars. The landslide portion of the model focused only on initiation sites for landsliding, whereas the surface erosion portion of the model included all areas with persistently exposed soils, regardless of the process by which vegetation was initially lost.

The new results reported here are consistent with and supersede the slpstab model; they provide greater resolution of erosion-prone areas based on watershed-specific landslide and erosion mapping.

Landslide Hazard Zonation Project

Mapping and field verification are not yet complete for the Dabob and Thorndyke watershed administrative units, which include the Tarboo/Dabob Bay watershed; however, a draft set of landforms and hazard ratings have been developed from the data collected so far (Jeff Grizzel and Ana Shafer, Jan 25, 2007 memorandum to Charlie Cortelyou and Al Vaughn). As stated in the Landslide Hazard Zonation Project Protocol (UPSAG 2006) "The LHZ (Landslide Hazard Zonation) Project was created to map potentially unstable slopes of the state. The goal of the LHZ Project is to eliminate errors of omission while identifying unstable landforms during the forest practices permitting process." The LHZ project protocol requires a detailed landslide inventory based on mapping from all available aerial photograph series, with field validation of some portion of the inventory. Based on the landslide inventory, it then requires the delineation of landforms, designed to "divide the landscape into geomorphically distinct areas sharing similar landform characteristics, forest practice sensitivity, and delivery potential". Based on the

landslide inventory, methods are specified to define hazard ratings for each landform based on the frequency of landslide occurrence, the area of landslides involved, and the degree of landslide delivery to public resources. Final products are a set of two maps, one of the landslide inventory, the other of potential landslide hazards, both at a 1:12,000 scale, and a written report. This protocol requires use of a consistent set of data sources, mapping techniques, data records, and analysis tools for all sites and all practitioners. The products are useful for anyone needing information on landslide processes and relative susceptibility.

Categorical hazard ratings (low, moderate, high, and very high) are defined for each landform type based on the relative frequency and area of mapped landslides associated with that landform. Hazard ratings provide a qualitative indication of relative susceptibility to landslide occurrence and delivery to a public resource. A low hazard rating does not indicate no potential for landslides, just a low potential relative to landforms with moderate and high ratings.

Although LHZ mapping and field verification are not complete for the watershed administrative units containing the Tarboo watershed, the Department of Natural Resources has provided data files showing the landslide inventory and draft landforms delineated to date. These are used here to show how the LHZ-delineated landforms and hazard rating might compare to results from the other types of slope stability mapping described in this report. Figure 14 shows draft delineated high-hazard landforms consisting of high-gradient slopes associated with incised channels, convergent headwalls, and coastal bluffs. For comparison, I show the area required to encompass 93% of the mapped shallow landslide initiation points and 93% of the exposed soils mapped for this study (93% is the proportion of mapped landslide sites included in high-hazard zones with slpstab, discussed above). Because LHZ mapping uses the same high-resolution data used here (1:12,000-scale aerial photography for landslide mapping, shaded relief image derived from 6-ft grid LiDAR DEM), landforms can be delineated with similar resolution. Thus LHZ mapping resolves inner gorges missed with lower-resolution data (e.g., 1:24,000-scale topographic data). Some high-hazard (93%) areas identified in this study are not included in LHZ-identified high-hazard landforms. This may result because LHZ hazard definitions include an assessment of the potential for landslide delivery to a public resource; a factor not included in the results from this study, which include only susceptibility to landslide initiation and, for surface erosion, susceptibility to persistent surface erosion after loss of vegetation. Likewise, in some areas, LHZ mapping included areas not identified as high-hazard zones for shallow landsliding using the methods in this study. This may reflect differences in mapping techniques. For LHZ landform mapping, boundaries are digitized by hand. In this study, high-hazard zones are identified, DEM cell by cell, using automated computer algorithms, which results in greater detail.

The techniques described here provide both high spatial resolution and a quantitative definition of susceptibility. Figure 15 shows the area required to encompass mapped landslide initiation and surface erosion sites by 1% increments. Hazard ratings can be defined to include any specified proportion of the mapped sites. This provides insight into the relative level of risk posed by

landsliding and surface erosion across the landscape. It also provides quantitative data that can be used with other models.

LHZ mapping of deep-seated landslides and associated groundwater recharge zones (Figure 16) illustrates the abundance of these features in the Tarboo watershed. In the draft LHZ mapping, these features are assigned an indeterminate hazard rating, indicating that remotely sensed information (aerial photographs, LiDAR) is insufficient for assessing hazards posed by these features. For the same reason, the techniques used in this study are unable to empirically quantify hazards posed by these deep-seated landslide features (see, however, further discussion below). LHZ mapping has not specifically identified earthflow terrain, which is incorporated as a component of the delineated deep-seated landslide features. Field observations (Figure 3) indicate that earthflows are active deep-seated processes (for at least two sites) within the watershed and, therefore, that efforts to identify earthflow terrain and to characterize the groundwater recharge zones that may influence earthflow activity are an important factor in assessment of landslide hazards. Figures 12 and 16 show the earthflow terrain identified with the automated procedure developed for this study, and approximate groundwater recharge zones to these sites based on surface topography. These hazard predictions must also be deemed "indeterminate"; topographic identification of earthflow terrain provides a hypothesis to be tested by field observations. These predictions provide an indication of the extent to which terrain indicative of earthflows, as resolved with the LiDAR elevation data, is found within the watershed.

Sensitivity to Land Use

To quantify sensitivity of landslide and erosion susceptibility to timber harvest, road building, and land conversions (e.g., from timber production to residential) requires that landslide inventories be divided between land-cover types (e.g., Miller and Burnett, 2007) for each time point that landslides are mapped. Such data were not available for this study, so what these results provide is a measure of topographic controls on landslide and erosion susceptibility (within areas underlain by deep glacial sediments). Nevertheless, we can use results from other studies to assess these results in terms of sensitivity to land uses.

Shallow-Rapid Landsliding

Loss of vegetation has several potential effects on hydrologic and other physical processes that determine susceptibility to landsliding. Root networks provide lateral and vertical interlocking between roots and with underlying substrates, acting to effectively increase soil strength (Schmidt et al. 2001, Roering et al. 2003). Theoretically, root strength therefore increases soil mass resistance to downslope movement. Timber harvest results in a decrease in root mass within the soil as roots decay over time (e.g., Schmidt et al., 2001), with an associated decrease in slope stability. Over time, as trees regrow and the root network expands, root reinforcement of the soil gradually increases. Hence, there is a period of time within the first decade or so after timber harvesting during which root reinforcement is reduced and landslide susceptibility

increased (Sidle 1992), consistent with on observed post-harvest increase in (shallow) landslide rates (Sidle and Ochiai 2006).

Forest canopy also acts as a transient holding zone for precipitation, reducing the peak intensity of precipitation falling to the ground during extreme rainfall events. Keim and Skaugset (2003), for example, found that measured peak rainfall intensities were damped up to 52% in a homogeneous 60-year-old managed stand in the Oregon Coast Range and up to 83% in an old-growth stand in the Gifford Pinchot national Forest in southwest Washington. High diffusivity soils (typically, those lacking extensive silt and clay, such as the outwash deposits in Tarboo watershed) can respond to high precipitation events with rapid and transient increases in pore pressure and associated loss of effective soil strength (Iverson 2000). The modulating effect of forest canopy on rainfall intensity may reduce the peak pore pressures associated with short-duration, high-intensity periods of rainfall. Loss of forest canopy may thereby increase susceptibility to shallow landsliding in response to high-intensity rainfall (Keim and Skaugset 2003).

Loss of root strength and loss of canopy storage may both act to increase landslide rates for some period after timber harvest. The degree of this increase is dependent on watershed-specific geotechnical factors and on the sequence of storm events that occur in the subsequent years. Studies at other sites provide an indication of the magnitude of this effect, but show a large range of variability. Robison et al. (1999) list a compendia of studies from the Pacific Northwest that report the ratio of landslide density in recently harvested to mature forests spanning a range from 0 to 30. None of these, however, were for areas with the stratigraphic legacy of continental glaciation that dominates landslide processes in the Tarboo watershed. In an unpublished report for the Stillaguamish Tribe, I reported landslide densities for deep glacial sediments in the Stillaguamish River basin (Miller 2004), which exhibit stratigraphy and material properties similar to those in the Tarboo/Dabob Bay study area. In that study, the spatial density of shallow-rapid landslides in deep glacial deposits were 20 times greater in unforested areas than in forested areas. For comparison, in areas underlain by bedrock, landslide density in unforested sites was only 4.5 times greater than in forested sites. These results accounted for differences in topography between these areas and suggests that unconsolidated glacial sediments exhibit greater sensitivity to loss of forest cover than areas underlain by bedrock.

Roads can also substantially increase landslide-related sediment fluxes. Roads affect landslide processes in several ways (Sidle and Ochiai 2006). Roads crossing hillslopes intercept surface and shallow subsurface drainage, which (in most cases) is routed along the road surface and in ditches to be discharged via culverts to the downslope side of the road. Improperly placed culverts and plugged or undersized ditches can concentrate water discharge onto downslope areas, causing increased susceptibility to landsliding (Montgomery 1994). Sidecast and road prism material placed on steep slopes can fail; cut slopes excavated for road construction can trigger both shallow landsliding of surficial material and activate deep-seated slumps.

Earthflows

Earthflows exhibit temporally and spatially variable rates of movement that respond to changes in geometry (e.g., stream undercutting of the toe or sides, slumping along the headscarp) and to changes in groundwater flux (e.g., Iverson and Major 1987). Depending on the geometry and material properties of the earthflow, response times can vary from days to years (Iverson 1986, 2000). Earthflow movements are naturally variable, responding for example to seasonal and annual variations in precipitation. The potential for land use to affect movement of earthflows in the Tarboo watershed hinge primarily on landuse-associated changes to groundwater flow. Loss of forest canopy reduces precipitation losses to evapotranspiration and increases rates of groundwater recharge, with associated increased water yield following timber harvest (Rothacher 1970). Harvest-related increases in groundwater flux to earthflows may then cause an increase in rates of earthflow movement. Swanston et al. (1988), for example, detected an increase in deformation rate following upslope clear-cut harvesting on an earthflow in southwest Oregon, which they attributed to elimination of canopy interception and evapotranspiration in the harvested area.

The potential for harvest-related reductions in interception and evapotranspiration to increase movement on deep-seated landslides (Miller and Sias 1998) has warranted specific recognition of groundwater recharge areas to deep-seated landslides in glacial sediments in the Washington State Forest Practices Board Manual (Chapter 16, Guidelines for Evaluating Potentially Unstable Slopes and Landforms, Section 5.4). Earthflows in the Tarboo/Dabob Bay watershed fall within this category. The groundwater recharge zone can be approximated using the drainage area to the landslide defined by surface topography. As shown in Figure 12, potential earthflow terrain is concentrated at the base of convergent headwalls formed in the outwash deposits. Thus, the groundwater recharge zone includes the entire headwall, potentially extending some distance onto the plateau beyond.

I am aware of no empirical data to quantify the likely consequences of harvest in this zone; for now we must rely on inferences based on current understanding of the processes involved. Changes in water yield tend to vary directly with the proportion of the recharge area harvested (Rothacher 1970) and increases in groundwater flow associated with loss of evapotranspiration are likely small compared to the variability associated with year to year variability in precipitation. Even so, modeling results (Miller and Sias 1998) suggest that harvest-related increases may substantially increase the time over which deformation occurs. The typically slow and gradual response of earthflows, with landuse effects overprinted on naturally variable rates of motion, can confound efforts to identify and quantify effects of landuse. That fact does not imply that such effects are inconsequential or can be ignored; rather, it suggests that a lack of evidence, based on currently available measures (e.g., air-photo mapping), is insufficient to demonstrate the absence of landuse effects.

Non-Earthflow Deep-Seated Landslides

As shown in the DNR landform mapping, topography indicative of large, deep-seated landslides encompasses a significant portion of the watershed. I found no evidence of recent activity on any of these landslides in the air photo mapping I did, and geotechnical reports for timber harvest applications in the watershed also report no evidence of recent activity on these features. As stated above in reference to earthflows, without the appropriate observations and measurements, lack of empirical evidence is not necessarily sufficient to demonstrate lack of landslide effects on landslide processes. What evidence would manifest activity of these features?

Topographic evidence of deep-seated landsliding is unequivocal, both with the LiDAR DEM and in field visits on the ground. Linear and arcuate scarps and benches lining numerous slopes outline the headscarps to these features; disrupted stratigraphy and hummocky topography identify downslope landslide debris. (I am referring now to areas distinct from the earthflow terrain). Lack of disrupted vegetation, lack of exposed soils in headscarps, and (in some cases) well-established drainage patterns all suggest little or no recent activity on these features. I am not aware of any catastrophic failures of any deep-seated landslides in the watershed. Lack of evidence for motion on these features suggests that they formed in response to conditions that do not currently exist (e.g., in response to rapid incision by glacial meltwater following ice-sheet retreat, in response to rising water tables following changing climate at the start of the Holocene), or that occur rarely (e.g., large-magnitude earthquakes). It does not imply that they will not move in the future. Given that this is a period of changing climate, with rising sea level, it is conceivable that changes in groundwater levels and rates of wave erosion can reactivate these features in coming years.

Consequences of Landsliding

An important aspect of all the methods for hazard zonation described in this report is that none consider the ultimate consequences to public resources. A complete assessment of risk should include an assessment of resource value and the consequences of landslide occurrence. This value and these consequences can vary spatially and temporally, so that the implications of a given susceptibility rating may also vary over space and time. This aspect of risk assessment is widely recognized, but tools for accomplishing it are not fully developed. Landslides and soil erosion are natural processes that provide crucial inputs to geomorphic and ecological processes. Landslides and soil erosion inevitably present two crucial and seemingly opposed functions: one is the destruction and degradation of existing habitat from burial or changes in texture (e.g., deposition of fine sediment in stream beds and littoral zones); the second is the creation and augmentation of habitat features (e.g., supply of spawning gravel and beach sand). The biota of ecosystems in landslide-prone terrain are well adapted to and dependent on these processes. They are also acutely sensitive to changes in the frequency and magnitude at which these processes occur (Reeves et al. 1995).

Tarboo/Dabob Bay presents one of the largest and least impacted saltwater marsh estuaries remaining in Puget Sound and as such, provides a unique combination of habitat components. At the same time, the bay provides prime real estate for growing oysters. At the northern end of Hood Canal, Tarboo/Dabob bay entails one component of an already at-risk saltwater body (see e.g., http://www.engr.washington.edu/epp/psgb/2007proceedings/papers/9a_newton_comp.pdf). The bay environments thus provide both ecologically and economically important functions for Washington State against which landslide and erosion hazards in the Tarboo watershed need to be assessed.

Activities that increase rates of sediment production and transport within the watershed will increase rates of sediment delivery to the bay. The fate of sediment in the bay depends largely on the mechanism of delivery. Landsliding and erosion of beach bluffs provide sources of beach sand and gravel (and large drift wood), subsequently carried by littoral drift to maintain the spits at the northern end of Dabob bay. In contrast, streams to the bay predominately carry fine-grained sediments. Tarboo bay in particular, containing lagoons protected by spits at its southern end, is a depositional site for stream-carried sediment and for sediment carried from Dabob Bay by the predominately northerly littoral drift, and is thus acutely sensitive to changes in the rate of sediment delivery. As discussed above, landslide susceptibility in glacial sediments is dramatically increased by loss of forest cover and construction of roads.

Sediment eroded from the watershed all ends up, eventually, in Tarboo Bay. Because the consequences of increased sediment production are concentrated there, the risks posed by activities at any one site in the watershed are conditioned by what has already occurred, or will occur, elsewhere. In this context, patterns of land ownership and associated land uses affect the risk posed by individual activities anywhere in the watershed. As larger proportions of the area susceptible to landsliding are precluded from activities that may increase erosion, the risk posed by activities elsewhere lessens. Set-aside areas are not immune to erosion, rather they increase the area over which these processes occur at natural rates. Evidence from other studies, discussed above, demonstrate that landslide rates in the soils and substrates that compose these slopes are particularly sensitive to loss of forest cover and road construction. It is logical, therefore, that a Natural Resource Conservation Area include areas where landsliding and subsequent soil erosion occur. The analyses presented here and in other studies demonstrate that these areas include all slopes draining to the bay and steep slopes adjacent to streams that drain to the bay.

REFERENCES

- Booth, D. B. and B. Hallet. 1993. Channel networks carved by subglacial water: observations and reconstruction in the eastern Puget Lowland of Washington. *Geological Society of America Bulletin* **105**:671-683.
- Booth, D. B., R. A. Haugerud, and K. G. Troost. 2003. The geology of Puget Lowland Rivers. Pages 14-45 in D. R. Montgomery, S. Bolton, D. B. Booth, and L. Wall, editors. *Restoration of Puget Sound Rivers*. University of Washington Press, Seattle, WA.

- Dunne, T. 1980. Formation and controls of channel networks. *Progress in Physical Geography* **4**:211.
- Grizzel, J. D. 2006. Geotechnical Assessment, "East Fork Tarboo" Timber Sale. Washington Department of Natural Resources, Olympia, WA.
- Iverson, R. M. 1986. Unsteady, nonuniform landslide motion: 2. Linearized theory and the kinematics of transient response. *Journal of Geology* **94**:349-364.
- Iverson, R. M. 2000. Landslide triggering by rain infiltration. *Water Resources Research* **36**:1897-1910.
- Iverson, R. M. and J. J. Major. 1987. Rainfall, ground-water flow, and seasonal movement at Minor Creek landslide, northwestern California: Physical interpretation of empirical relations. *Geological Society of America Bulletin* **99**:579-594.
- Keim, R. F. and A. E. Skaugset. 2003. Modelling effects of forest canopies on slope stability. *Hydrological Processes* **17**:1457-1467.
- McKean, J. and J. Roering. 2004. Objective landslide detection and surface morphology mapping using high-resolution airborne laser altimetry. *Geomorphology* **57**:331-351.
- Miller, D. J. 2004. Landslide Hazards in the Stillaguamish Basin: A New Set of GIS Tools. The Stillaguamish Tribe of Indians.
- Miller, D. J. and K. M. Burnett. 2007. Effects of forest cover, topography, and sampling extent on the measured density of shallow, translational landslides. *Water Resources Research* **43**.
- Miller, D. J. and J. Sias. 1998. Deciphering large landslides: linking hydrological, groundwater and slope stability models through GIS. *Hydrological Processes* **12**:923-941.
- Montgomery, D. R. 1994. Road surface drainage, channel initiation, and slope instability. *Water Resources Research* **30**:1925-1932.
- Montgomery, D. R. and W. E. Dietrich. 1994. A physically based model for the topographic control on shallow landsliding. *Water Resources Research* **30**:1153-1171.
- Pierson, A. 2004. Geologic Report: Slope stability assessment of the Golden Goat Timber Sale. Washington Department of Natural Resources, Olympia, WA.
- Reeves, G. H., L. E. Benda, K. M. Burnett, P. A. Bisson, and J. R. Sedell. 1995. A disturbance-based ecosystem approach to maintaining and restoring freshwater habitats of evolutionarily significant units of anadromous salmonids in the Pacific Northwest. Pages 334-349 in J. L. Nielson and D. A. Powers, editors. *Evolution and the Aquatic Ecosystem: Defining Unique Units in Population Conservation*, American Fisheries Society Symposium 17. American Fisheries Society, Bethesda, Maryland, USA.
- Robison, G. E., K. A. Mills, J. Paul, L. Dent, and A. Skaugset. 1999. Storm impacts and landslides of 1996: final report. Forest Practices Technical Report 4, Oregon Department of Forestry, Salem, OR.
- Roering, J. J., J. W. Kirchner, and W. E. Dietrich. 2005. Characterizing structural and lithologic controls on deep-seated landsliding: Implications for topographic relief and landscape evolution in the Oregon Coast Range, USA. *Geological Society of America Bulletin* **117**:654-668.
- Roering, J. J., K. M. Schmidt, J. D. Stock, W. E. Dietrich, and D. R. Montgomery. 2003. Shallow landsliding, root reinforcement, and the spatial distribution of trees in the Oregon Coast Range. *Canadian Geotechnical Journal* **40**:237-253.
- Rothacher, J. 1970. Increases in water yield following clear-cut logging in the Pacific Northwest. *Water Resources Research* **6**:653-658.

- Schmidt, K. M., J. J. Roering, J. D. Stock, W. E. Dietrich, D. R. Montgomery, and T. Schaub. 2001. The variability of root cohesion as an influence on shallow landslide susceptibility in the Oregon Coast Range. *Canadian Geotechnical Journal* **38**:995-1024.
- Shaw, S. C. and D. H. Johnson. 1995. Slope morphology model derived from digital elevation data. Northwest ARC/INFO Users Conference, Coeur d'Alene, ID.
- Shaw, S. C. and L. Vaugeois. 1999. Comparison of GIS-based Models of Shallow Landsliding for Application to Watershed Management. TFW-PR10-99-001, Washington Department of Natural Resources, Forest Practices Division, Olympia, WA.
- Sidele, R. C. 1992. A theoretical model of the effects of timber harvesting on slope stability. *Water Resources Research* **28**:1897-1910.
- Sidele, R. C. and H. Ochiai. 2006. *Landslides Processes, Prediction, and Land Use*. American Geophysical Union.
- Swanston, D. N., G. W. Lienkaemper, R. C. Mersereau, and A. B. Levno. 1988. Timber harvest and progressive deformation of slopes in southwestern Oregon. *Bulletin of the Association of Engineering Geologists* **25**:371-381.
- UPSAG. 2006. *Landslide Hazard Zonating Project Protocol*. Washington Department of Natural Resources, Olympia.
- Wieczorek, G. F. 1987. Effect of rainfall intensity and duration on debris flows in central Santa Cruz Mountains, California. Pages 93-104 *in* J. E. Costa and G. F. Wieczorek, editors. *Debris Flows / Avalanches: Process, Recognition, and Mitigation*. The Geological Society of America, Boulder, CO.

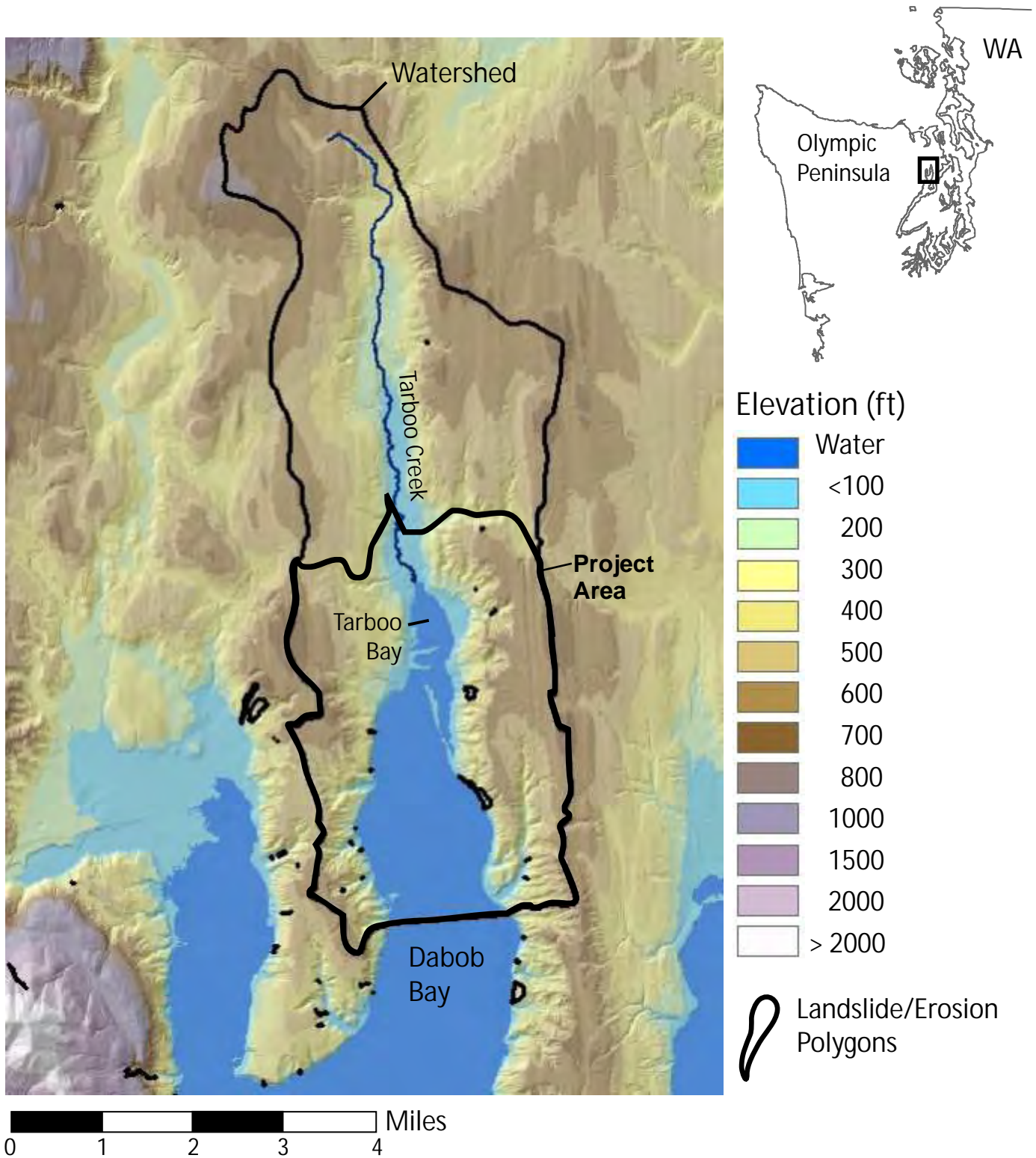
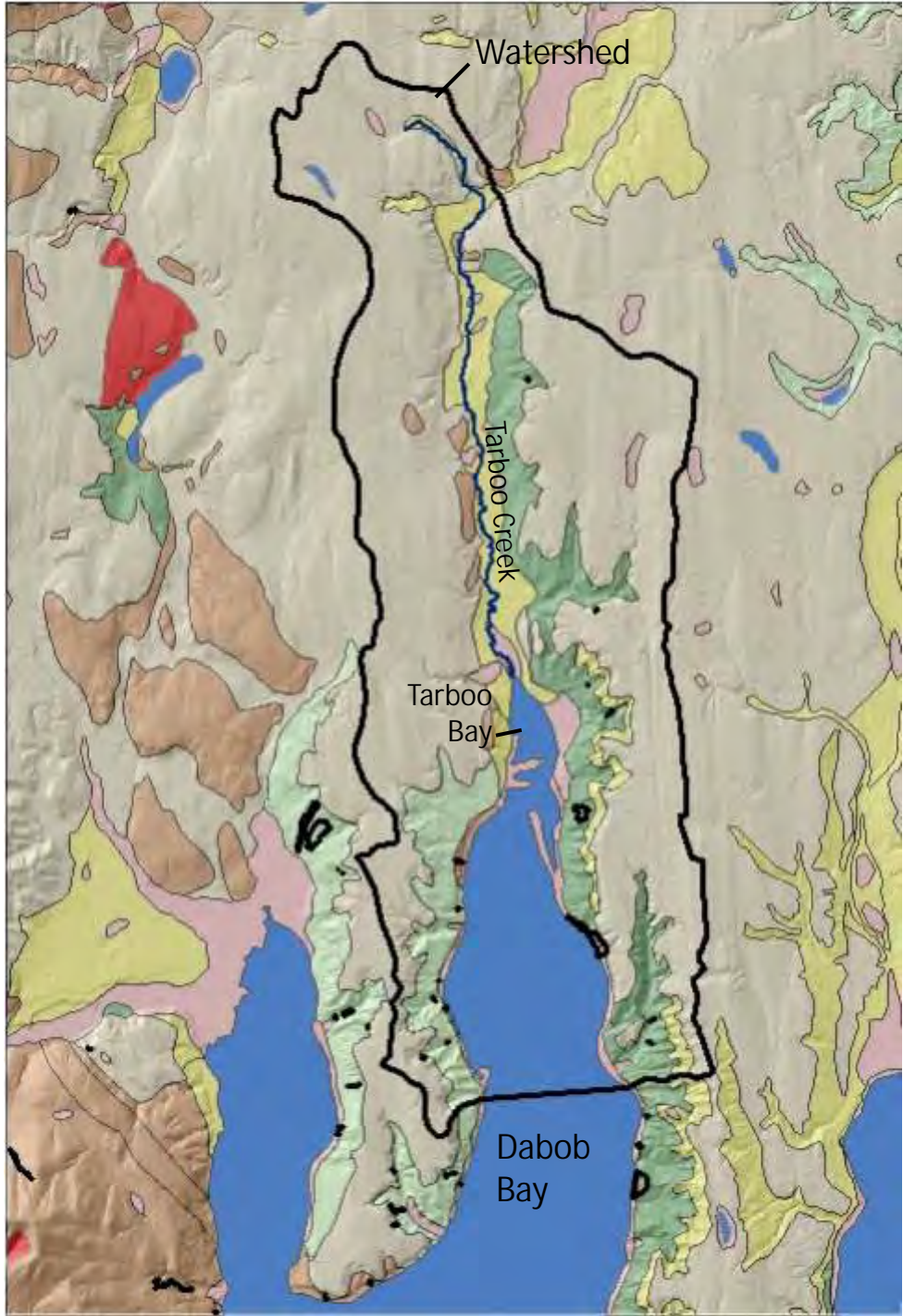


Figure 1. Study area, including the Tarboo watershed. Mapped landslide and surface erosion polygons used for model calibration are shown.



Generalized Geology
 (from WA DNR, OFR 2005-3,
 1:100,000 scale digital map)

Glacial Deposits

- Outwash
- Older Deposits
- Undifferentiated
- Till

Other

- Alluvium
- Bedrock
- Landslide Deposits

Landslide/Erosion Polygons

0 1 2 3 4 Miles

Figure 2. Generalized geology of the study area. Mapped landslides occur almost entirely within areas mapped as glacial outwash and older or undifferentiated glacial sediments.



Figure 3. Earthflow terrain is characterized by discontinuous zones of slumping and downslope soil creep, indicated by disturbed vegetation, as seen in the photograph above, and exposed soils at headscarps of small slumps, as seen in the photo at left.

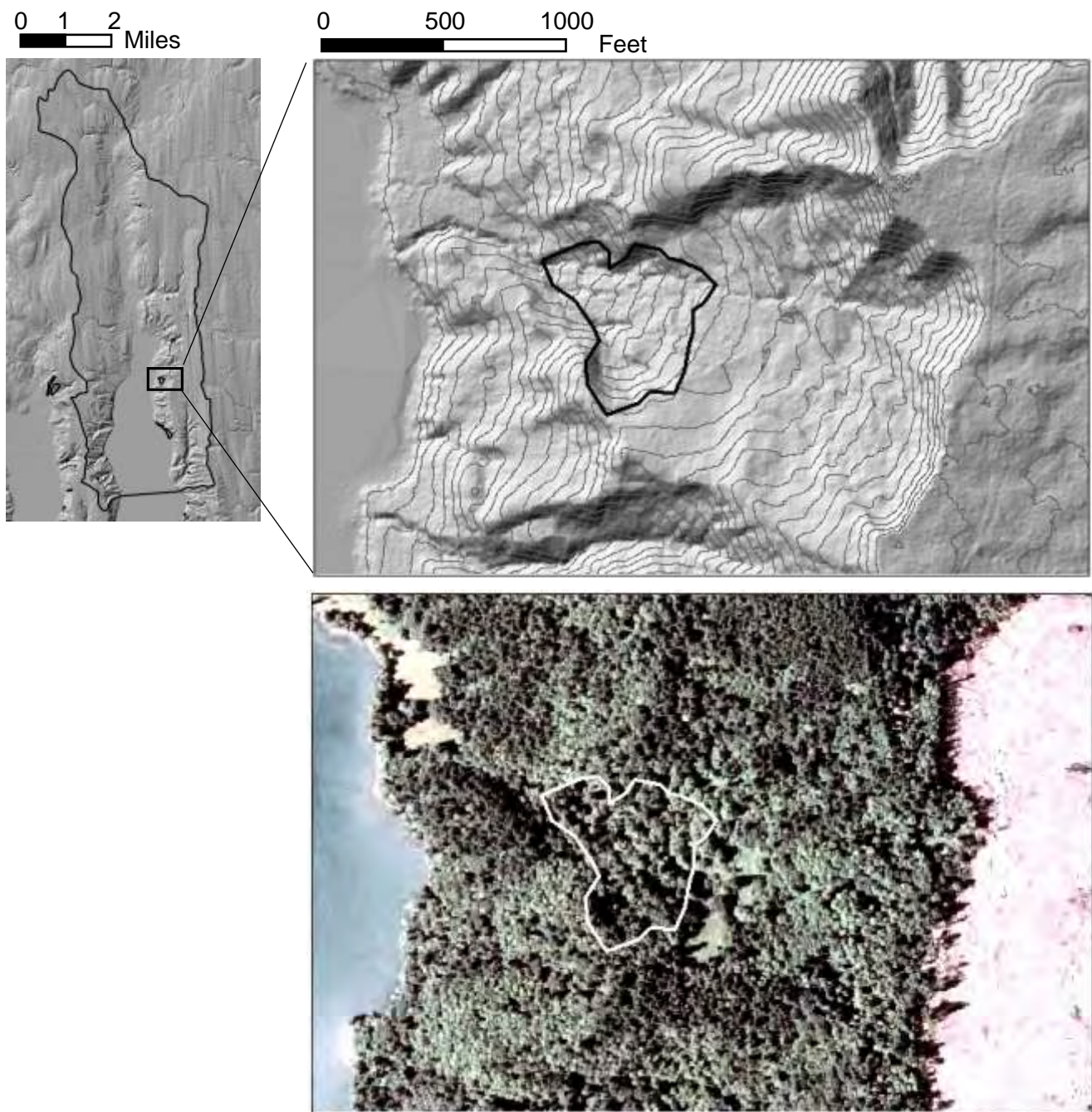
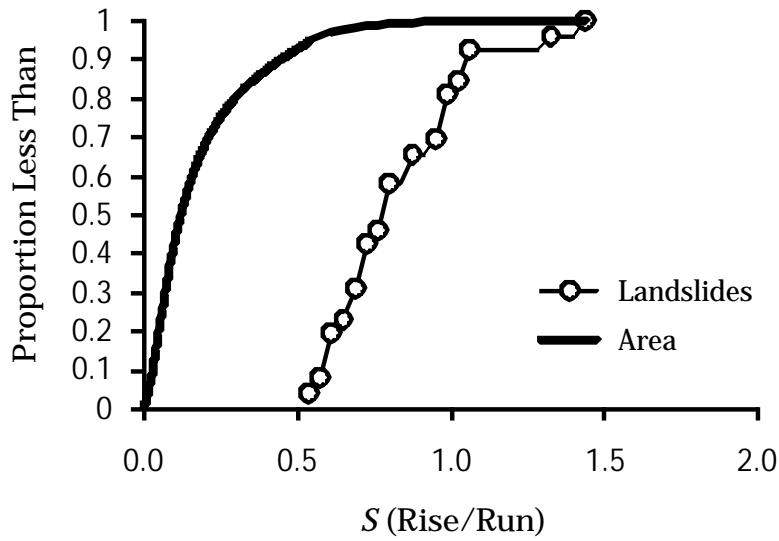


Figure 4. Mapped earthflow identified from disrupted vegetation in 1979 photograph. Upper image shows LiDAR-derived shaded relief image, with 10-foot contour lines. The dark line indicates the estimated extent of the active earthflow on the 1979 photo. The lower image shows the same area on the 2006 NAIP imagery. There is no obvious indication of the inferred earlier earthflow activity in the vegetation. However, there is a slightly increased surface roughness evident within the earthflow on the shaded relief image.

a) Slope (S)



b) Slope*Convergence (Sb)

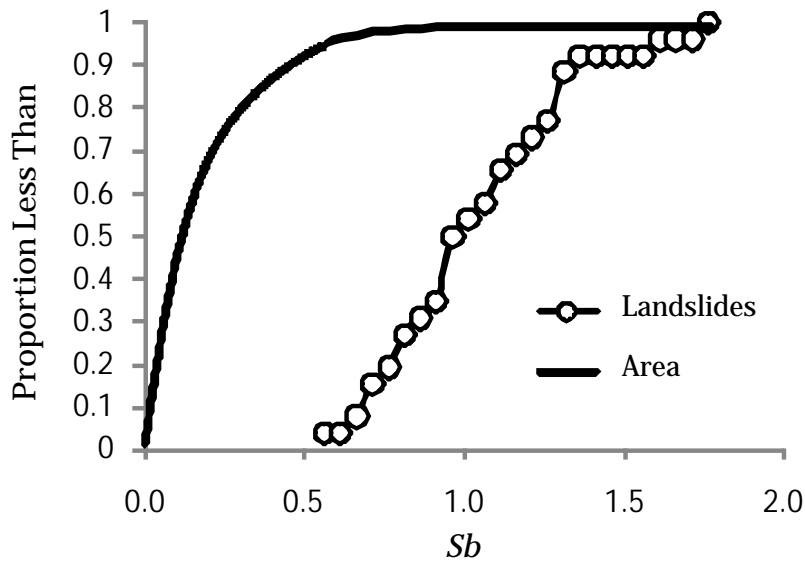
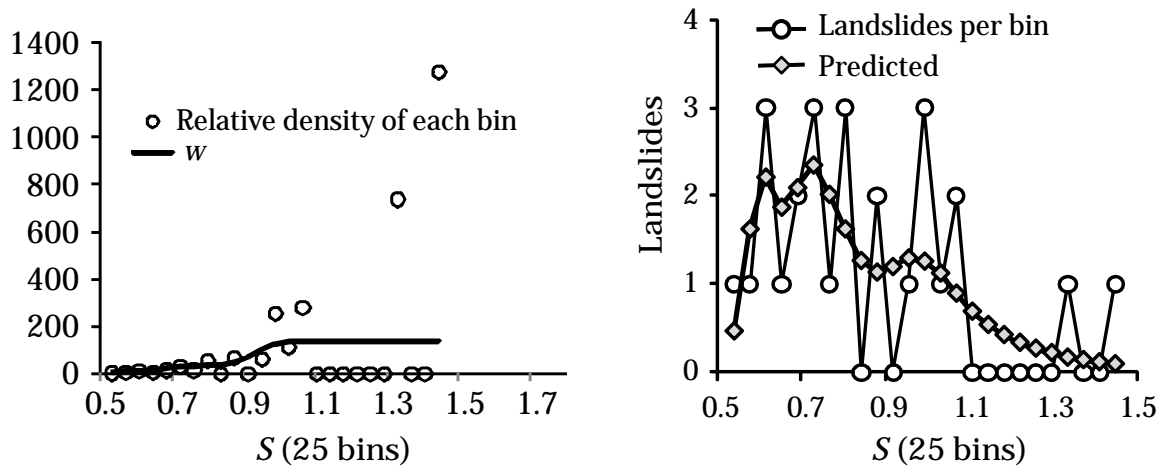


Figure 5. Cumulative distribution of area and mapped shallow landslides within the study area plotted against a) slope (S) and b) slope times topographic convergence (Sb).

a) Slope (S)



b) Slope*Convergence (Sb)

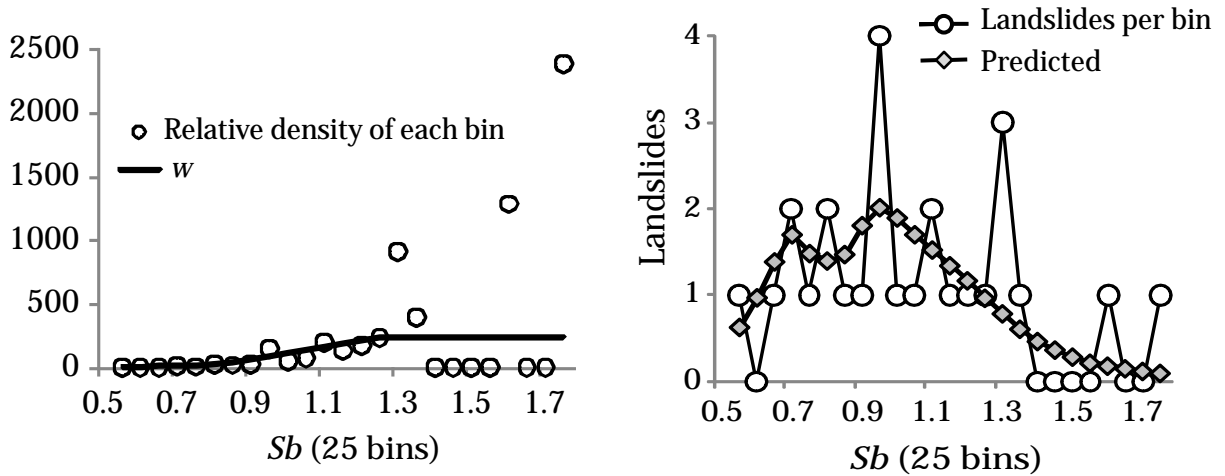


Figure 6. The left graphs show the relative landslide density (Eq. 2) for each bin and the topographic weighting function w fit to minimize differences between the observed and predicted number of landslides in each bin, shown in the right graphs, based on a) slope (S), and b) slope times topographic convergence (Sb)

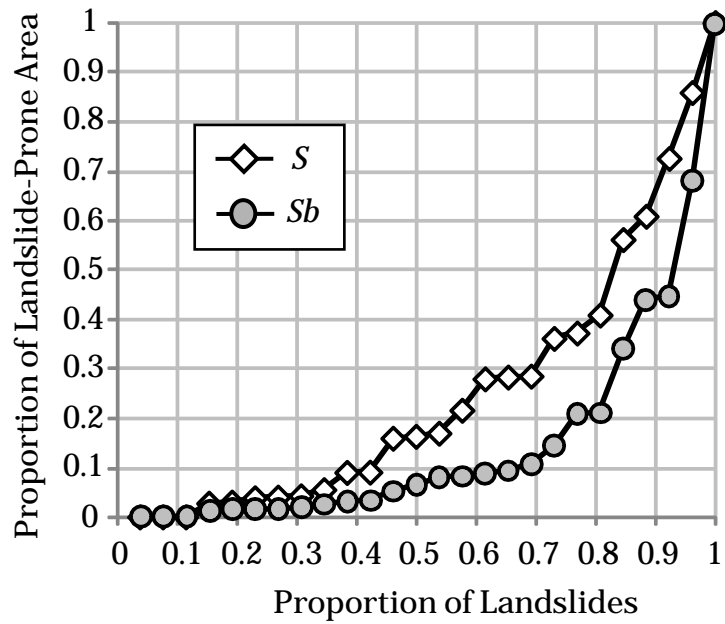
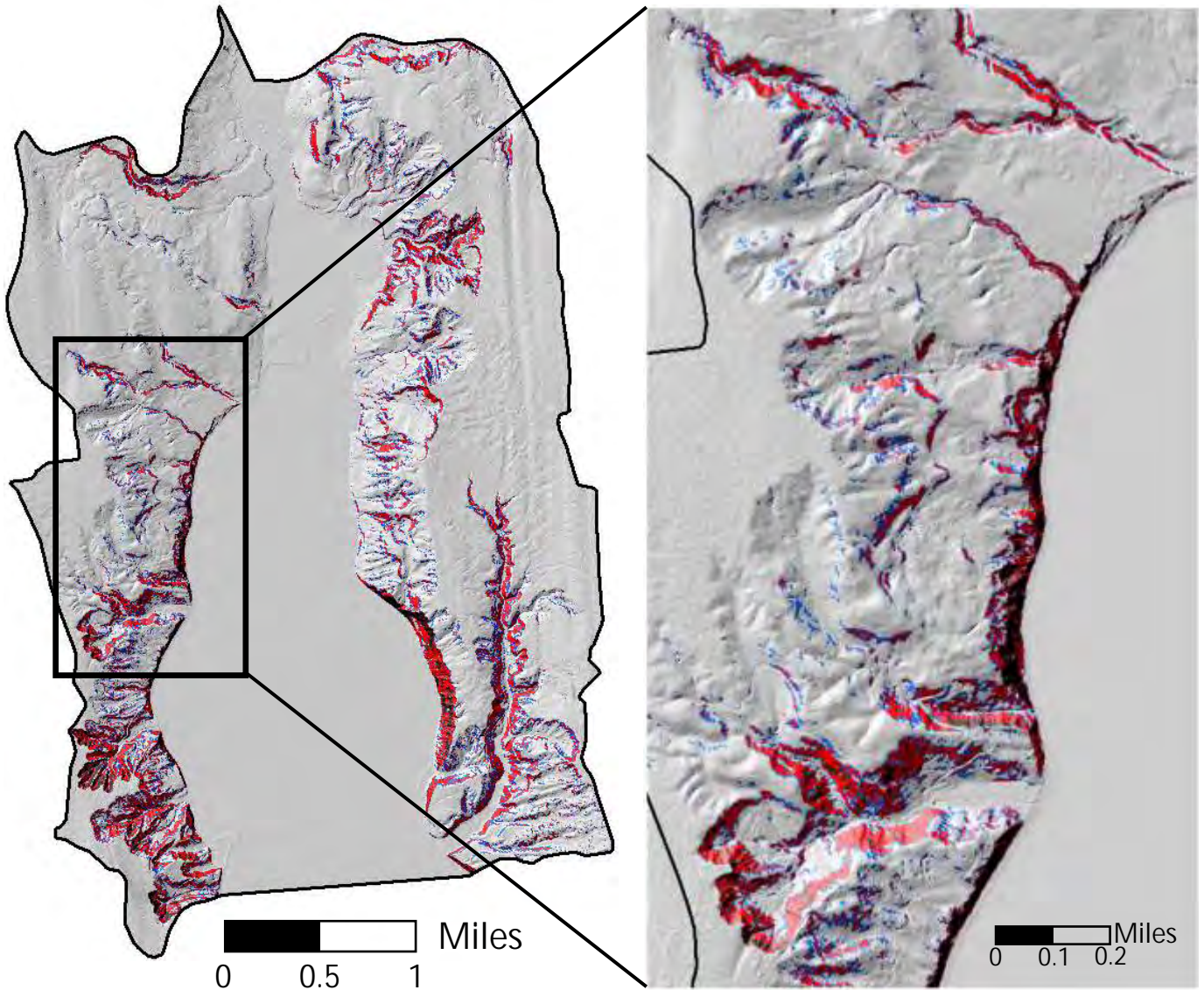


Figure 7. Using the topographic weighting functions shown in Figure 4, the proportion of watershed area required to encompass a given proportion of the expected landslides is plotted for both the slope (S) and slope-times-convergence (Sb) based criteria.



Shallow Landslide Susceptibility

- > 93 - 100%
- > 50 - 93%
- 50% of landslide initiation sites

Figure 8. Susceptibility to shallow landsliding from combined slope (S) and slope-times-convergence (Sb)-based topographic weighting. Susceptibility is characterized in terms of the percentage of landslide initiation points included in each zone (color). Red and black combined encompass 93% of all mapped landslides, the same proportion included in the high hazard rating used by the DNR slpstab slope-stability screen.

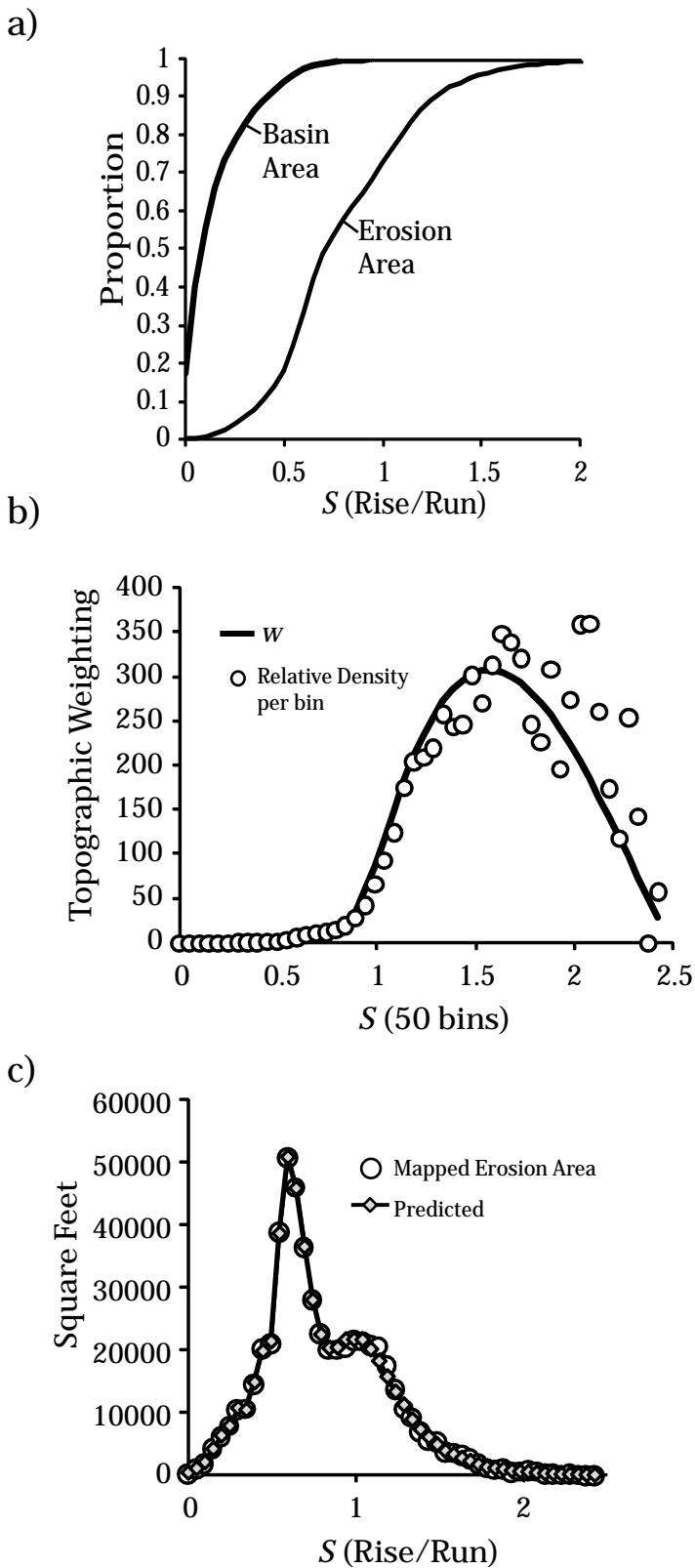
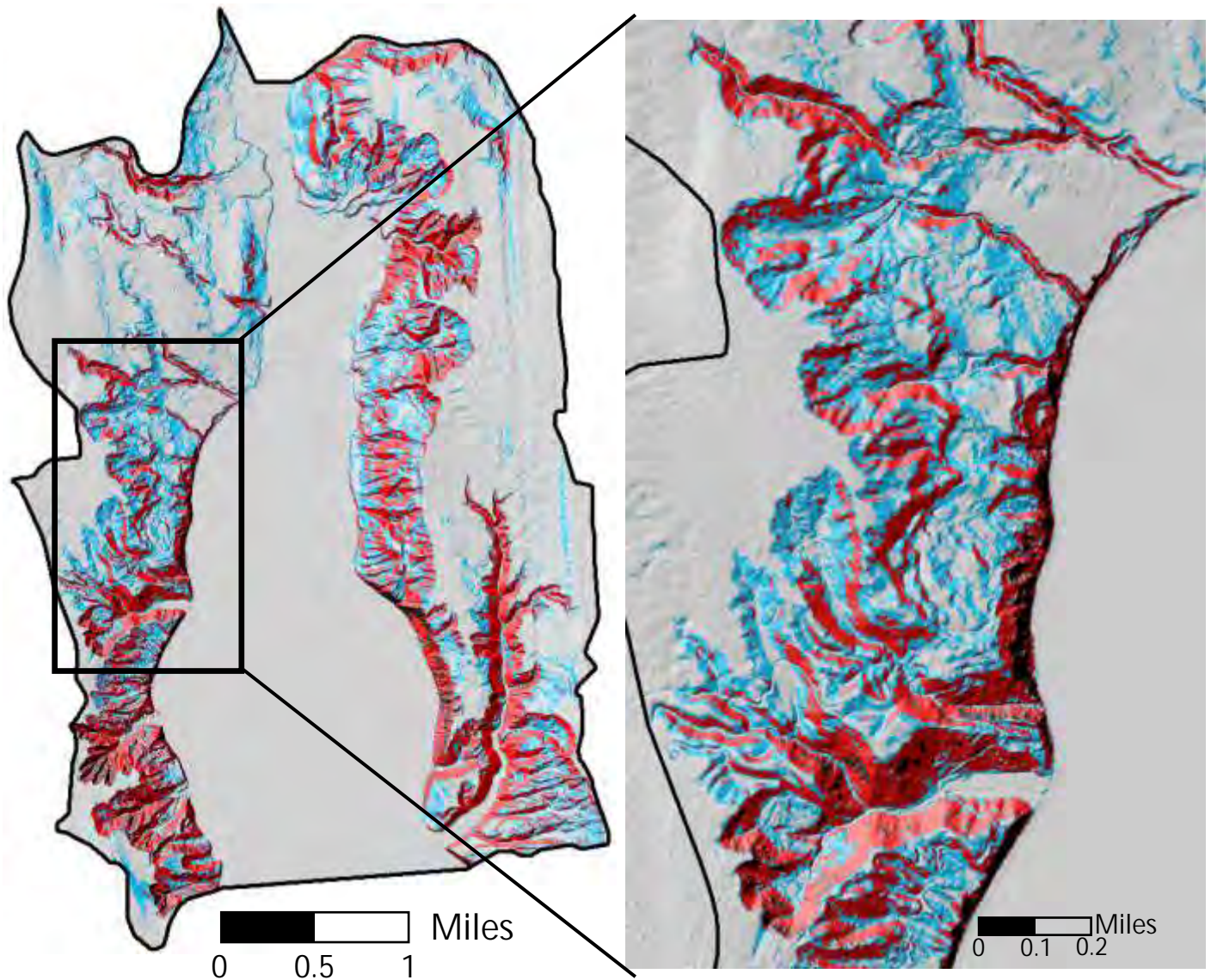


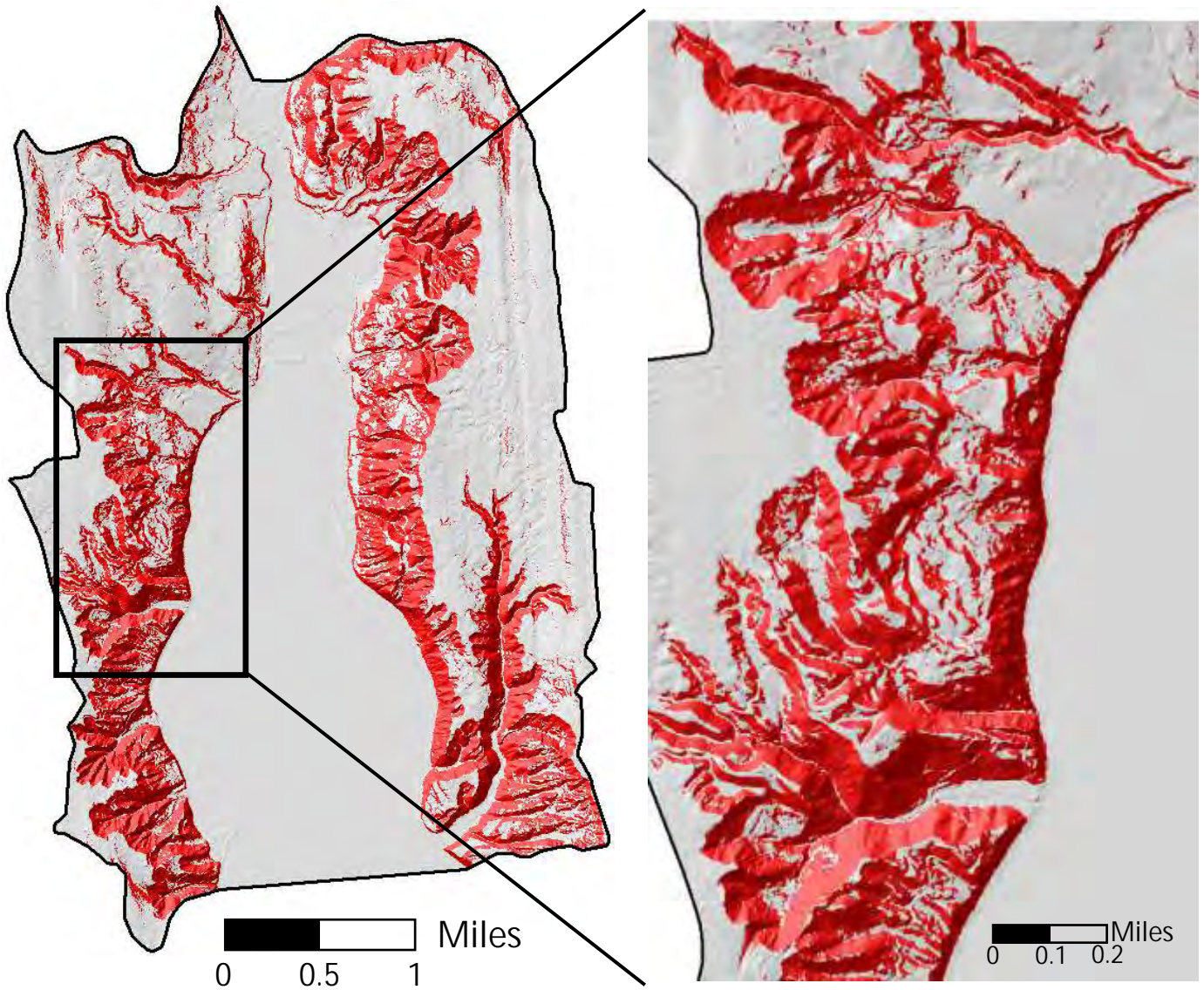
Figure 9. Surface Erosion: a) Cumulative distribution of basin area and mapped erosional sites plotted against surface slope (S), b) the resulting relative density and calibrated weighting function, and c) the observed and predicted area of active surface erosion in each bin.



Susceptibility to Erosion of Exposed Soils

- > 93 - 99%
- > 50 - 93%
- 50% of landslide initiation sites

Figure 10. Susceptibility to surface erosion calibrated to slope gradient. Susceptibility is characterized in terms of the percentage (by area) of actively eroding sites mapped on aerial photographs included in each zone (color). Red and black combined encompass 93% of the total area of all mapped erosional sites, the same proportion included in the high landslide hazard rating used by the DNR slpstab slope-stability screen.



Susceptibility to Landsliding and Erosion

99% of all mapped sites

Figure 11. Combined susceptibility to shallow landsliding and erosion of exposed soils. Red zones encompass essentially all landslide and erosion-prone areas, based on air photo mapping of such sites correlated to topographic attributes.

Figure 12. A topography-based estimate of earthflow terrain locations, using surface roughness, average slope, and convergence. Terrain characteristics were calculated over a 300-foot radius. Contributing area serves as an estimate of the groundwater recharge area to the zones.

- 25% area meets earthflow criteria
- 50% area meets earthflow criteria
- Contributing area to 25% zones
- Contributing area to 50% zones

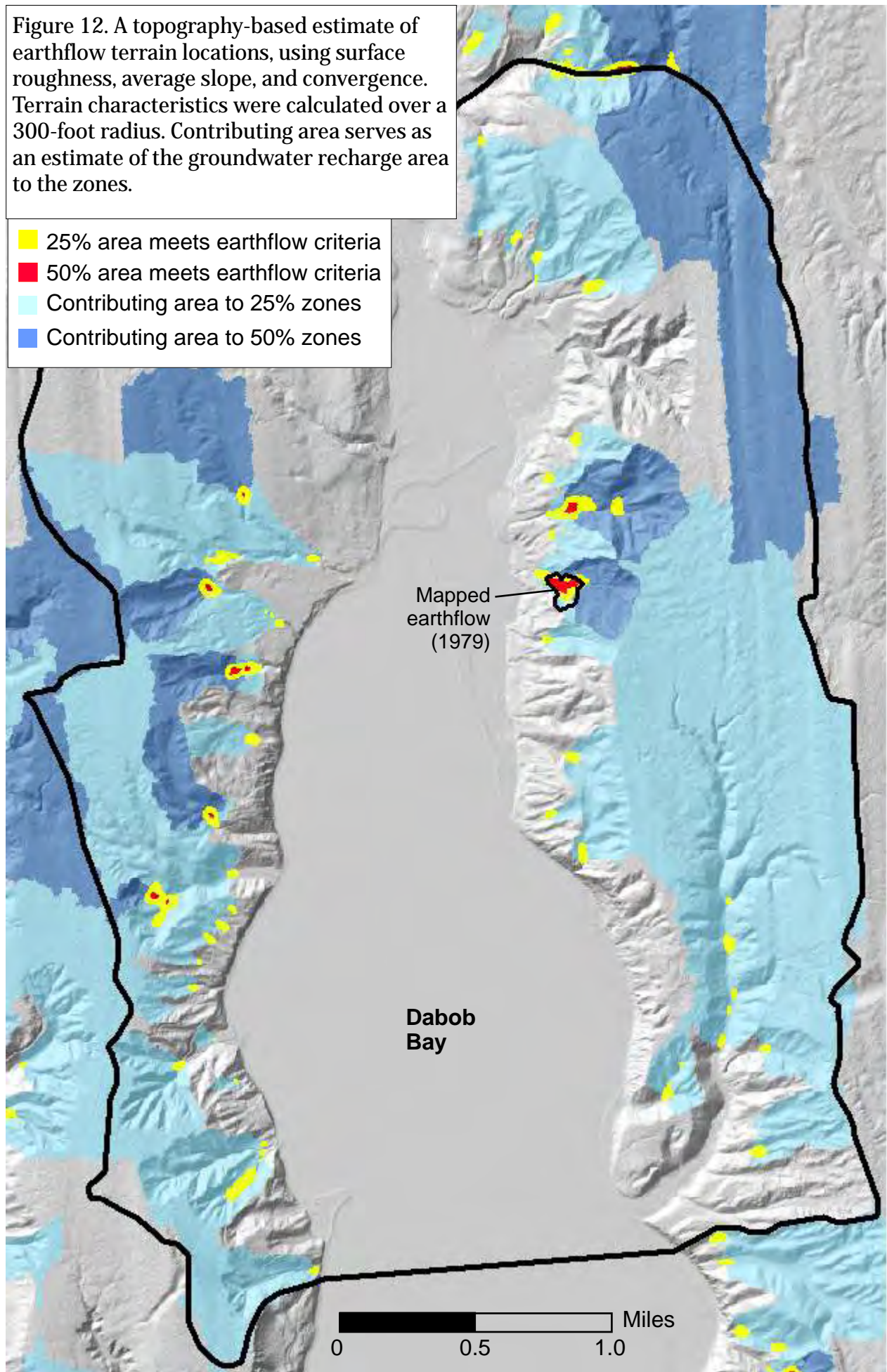
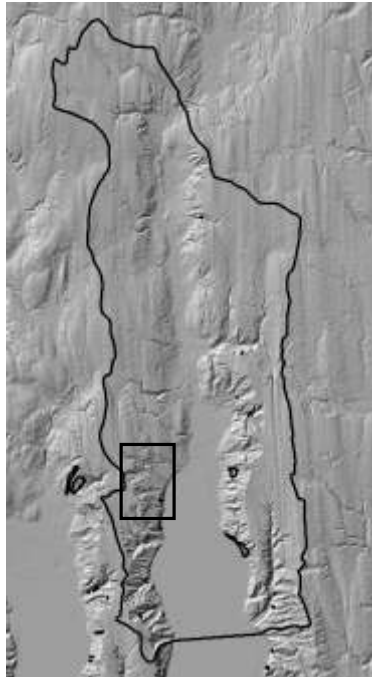


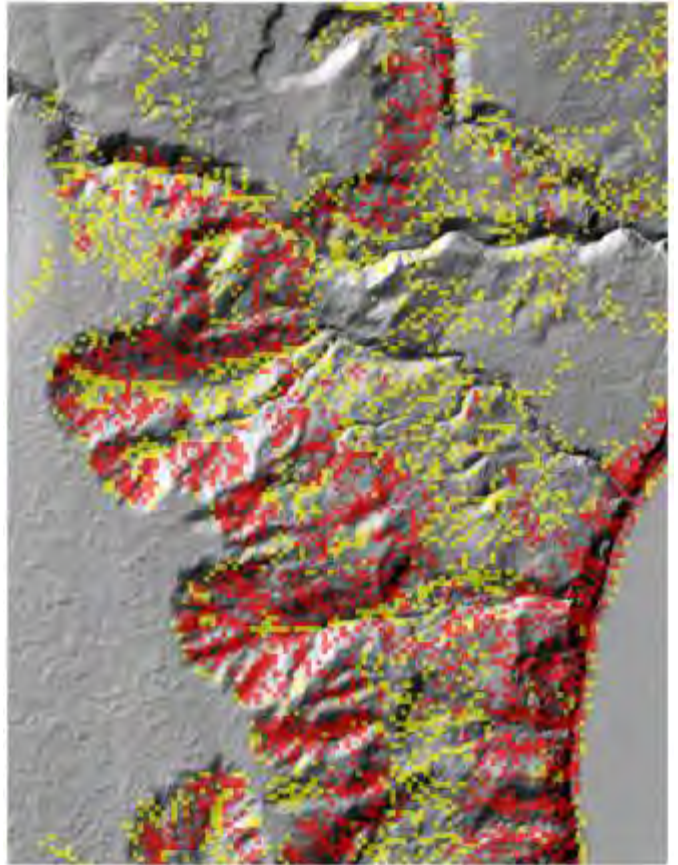
Figure 13. Comparison of DNR's slpstab modeled slope stability screen and results from this study. High-hazard zones include 93% of the mapped landslide sites used to calibrate these models.

0 1 2 Miles

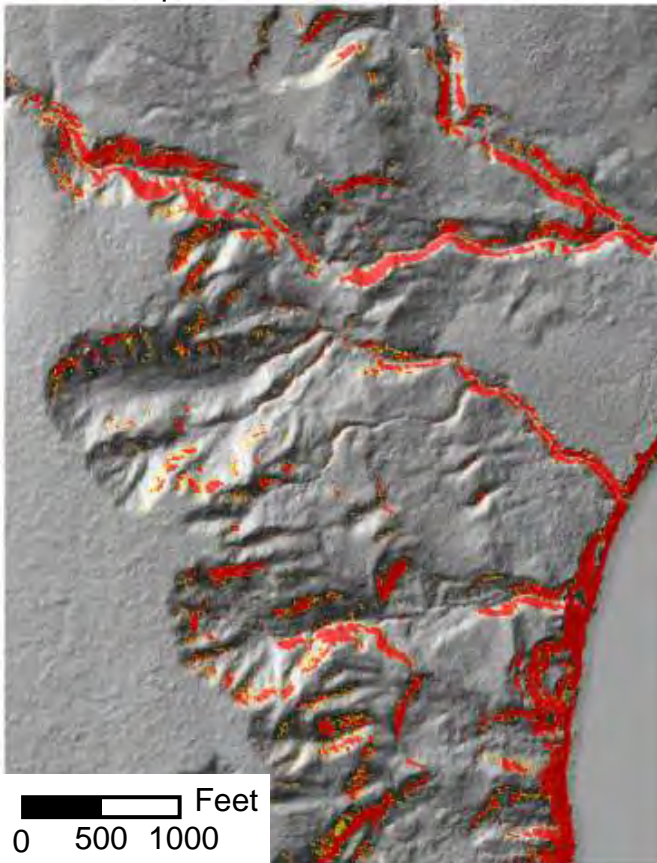


Hazard
■ Moderate
■ High

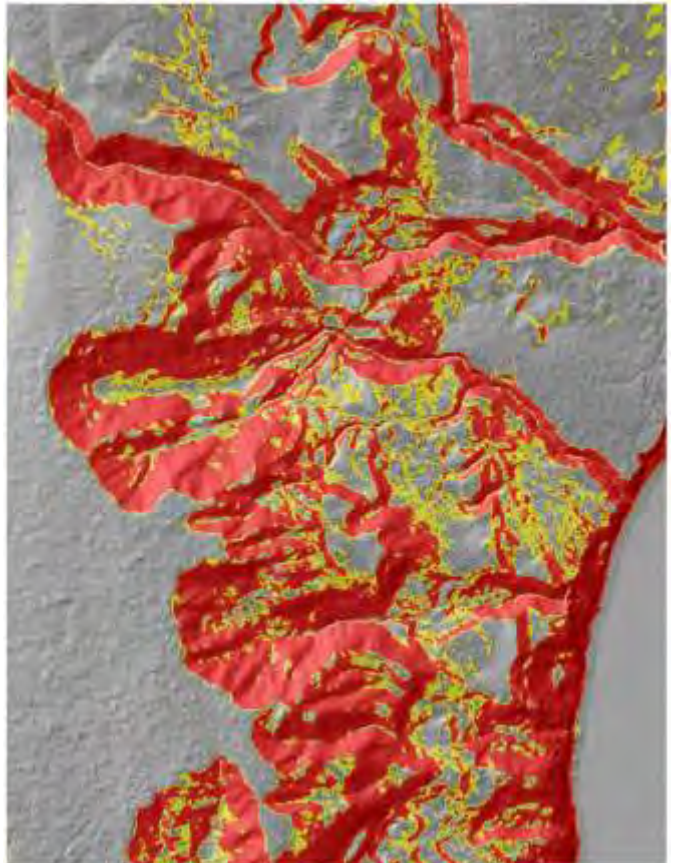
DNR slpstab



Shallow-rapid landslides



Shallow-rapid landslides + surface erosion



A. LHZ Landform: High-gradient slopes associated with incised channels, convergent headwalls, and coastal bluffs

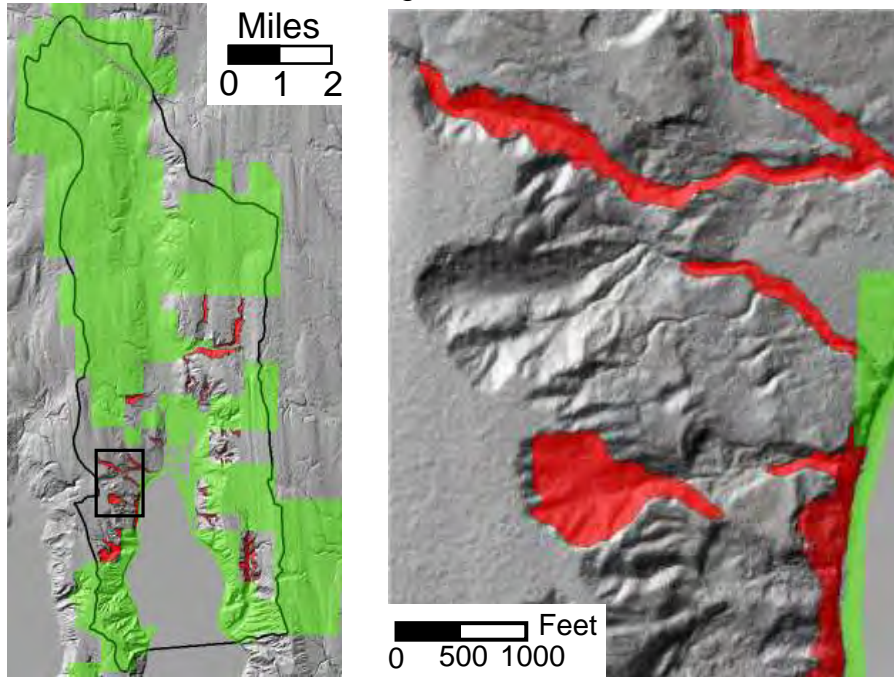
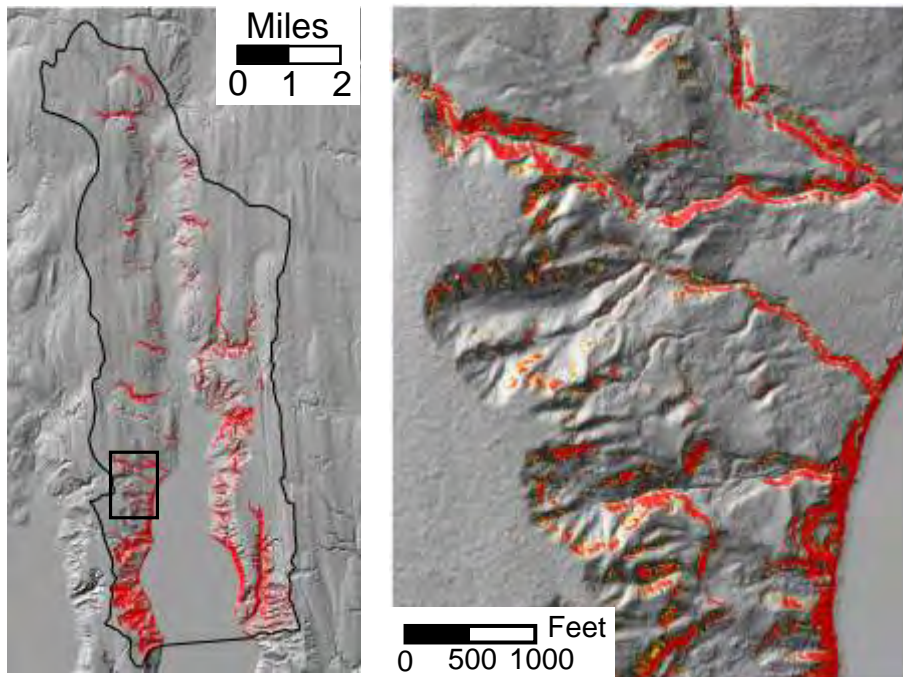
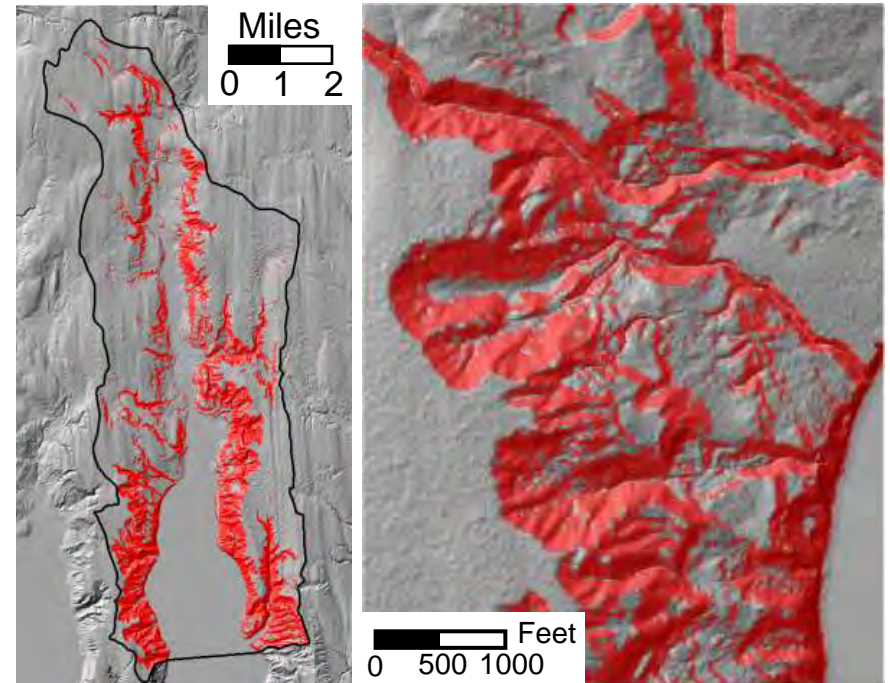


Figure 14. Draft LHZ landforms provided by DNR for state-owned lands (A) compared with high-hazard zones for shallow landsliding (B) and surface erosion (C) identified with this study. Green shading in Figure A indicate privately owned lands, for which LHZ landform mapping has not yet been started.

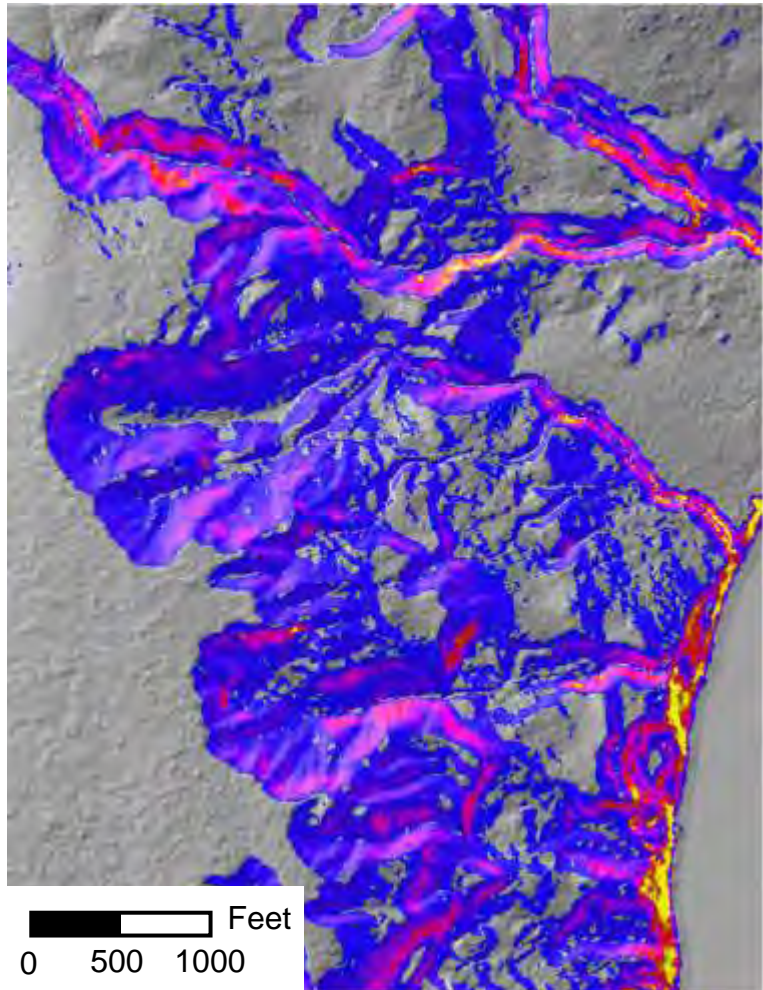
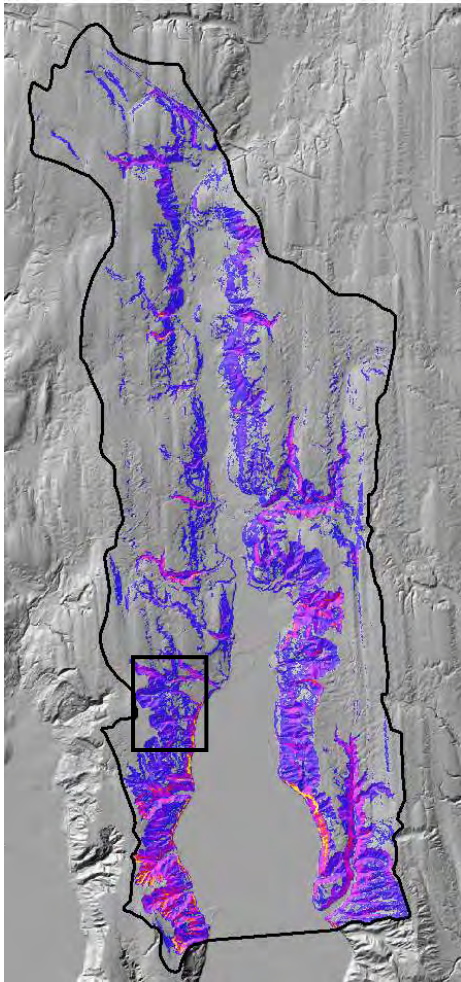
B. Areas encompassing 93% of mapped landslides



C. Areas encompassing 93% of mapped landslides and surface erosion



0 1 2 Miles



Proportion of Mapped Sites Included

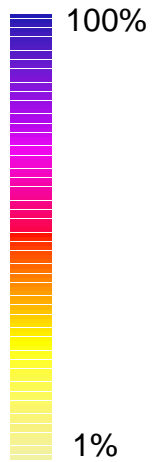


Figure 15. Susceptibility to landsliding and surface erosion is quantified along a continuous scale, based on the proportion of the mapped landslide and surface erosion sites mapped that are encompassed within the area delineated, starting with the least stable sites (yellow) and progressing to the most stable (blue).

A. LHZ Deep-seated landslides and groundwater recharge zones

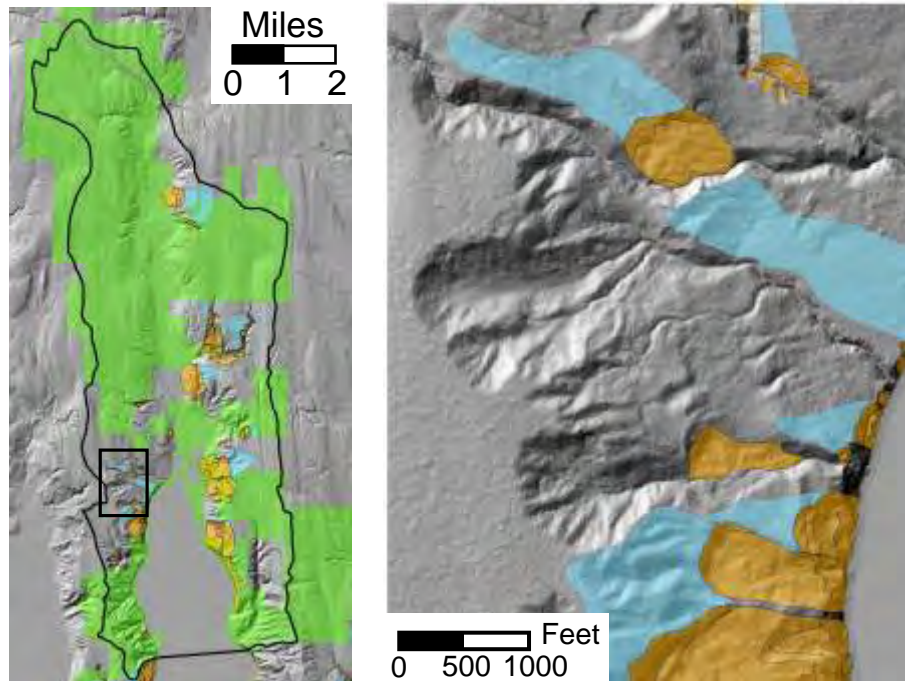
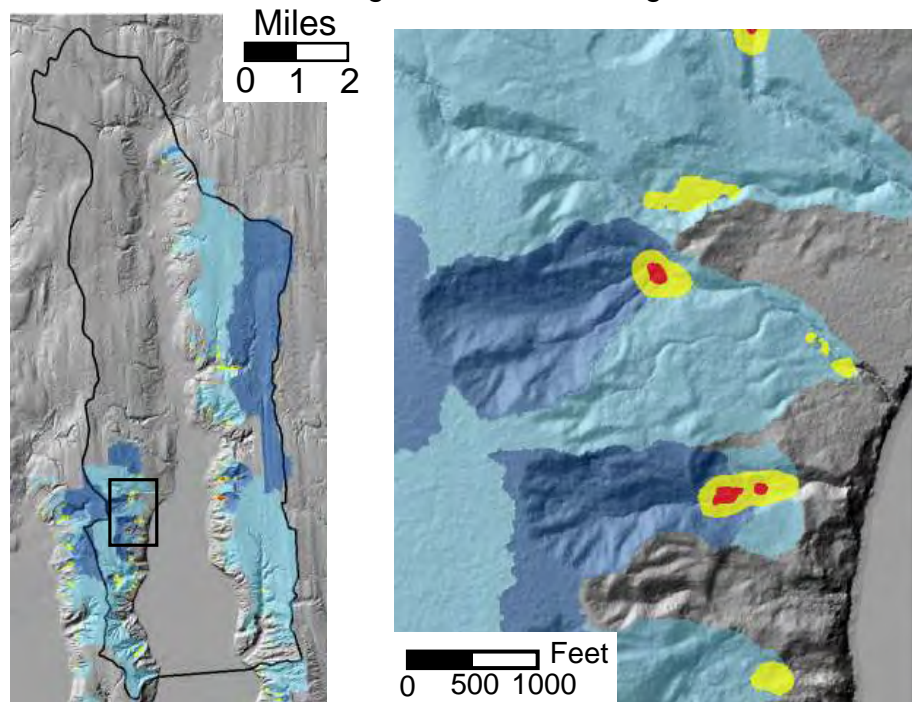


Figure 16. LHZ deep-seated landslides and groundwater recharge zones (A) compared to potential earthflow terrain and associated groundwater recharge zones identified in this study (B). Note that the LHZ landform delineations are incomplete and in draft form; these are presented only to illustrate similarities and differences between these techniques.

- Deep-seated landslide
- Groundwater recharge zone

B. Earthflow terrain and groundwater recharge zones



- 25% area meets earthflow criteria
- 50% area meets earthflow criteria
- Contributing area to 25% zones
- Contributing area to 50% zones